2017

Quantifying the Interactions of Nickel with Marine Dissolved Organic Matter Using Fluorescence

Elissa Dow
Wilfrid Laurier University, dowx8600@mylaurier.ca

Quantifying the Interactions of Nickel with Marine Dissolved Organic Matter Using Fluorescence

By

Elissa Dow

Honours B.Sc. Chemistry, University of New Brunswick, 2013

THESIS

Submitted to the Department of Chemistry and Biochemistry

Faculty of Science

in partial fulfilment of the requirements for

Master of Science in Chemistry and Biochemistry

Wilfrid Laurier University

2017

Abstract

Nickel (Ni) is a versatile metal with an abundance of applications, namely its role in stainless steel, electronics, and batteries, making it a popular choice in industry. Unfortunately, with increasing demand and production comes higher amounts of Ni pollution. Nickel enters ocean waters - either directly or indirectly - and can have profound effects on marine life. Nickel has been established as a toxicant to a variety of aquatic biota, with the divalent cation (Ni^{2+}) thought to be the most bioavailable fraction and thus the most toxic. Having a reliable means of quantifying free Ni ion is pertinent toward establishing appropriate water quality recommendations for aquatic life protection. The objective of this study was to compare two speciation techniques to quantify Ni^{2+} in natural samples. The methods studied in this work were ion-selective electrode (ISE) and fluorescence quenching (FQ) titrations.

Results indicated that a Ni-ISE is more easily applicable in low ionic strength samples since electrode potential changes to added Ni were only seen in freshwater. Fluorescence excitation-emission matrices were scanned to identify fluorophores within the samples, and variable angle synchronous spectra were used to monitor titrations. Binding constants (log K) as well as complexing capacities (L_T) were derived using nonlinear regression, and Monte Carlo analysis was used to relate these values to EC_{50} Ni levels from toxicity tests (conducted by a collaborative group) on the same samples. Results showed that the predicted Ni^{2+} concentrations at EC_{50} levels had overlapping 95% confidence intervals for *Mytilus edulis*. The free Ni^{2+} concentration did not overlap for *Strongylocentrotus purpuratus*, though it should be noted that there was only one data point. The *Mytilus edulis* results also agreed with the artificial seawater (ASW) control, highlighting the validity and usefulness of a Biotic Ligand Model (BLM) for marine Ni.

Acknowledgements

The past few years were challenging, but there were several people along the way who helped me accomplish what I had started to believe was not possible.

Firstly, I would like to thank my supervisor, Dr. Scott Smith, for providing me with this opportunity. I wanted to pursue a graduate degree, and you allowed me to do this. Thank you for retaining faith in me since my first day in Waterloo.

Thank you to Dr. Jim McGeer and Dr. Vladimir Kitaev, whose comments and questions during committee meetings exercised my brain. I appreciate you both taking the time to be on my committee. And thank you to Dr. Michael Suits for agreeing to be my external examiner.

Thanks to the CLEAR lab members who showed me the ropes, and thanks to those who directly helped with data for my project: Alex Carvajal for ISE-troubleshooting, and Dr. Tamzin Blewett for sharing toxicity results.

A special thank you goes to Gena Braun for her immense amount of patience and technical expertise.

To my friends, new and old, I am grateful for your support – both academically and outside of school. I appreciate everyone who has helped me to move forward.

To my family: you mean more to me than everything. Thank you for never pressuring me, and for allowing me to choose my own path. Your endless confidence and care is the reason I made it to the other side of this degree.

Lastly, I want to thank the organizations who funded this project, both directly and indirectly: CDA (Copper Development Association), HyrdoQual Laboratories Ltd., ICA (International Copper Association), ILZRO (International Lead and Zinc Research Organization), IZA (International Zinc Association), NiPERA (Nickel Producers Environmental Research Association), and NSERC, Teck Resources Inc., Vale Canada, and Xstrata Zinc.

List of Abbreviations

BLM	Biotic Ligand Model
CCME	Canadian Council of Minister of the Environment
CI	Confidence Interval
DOC	Dissolved Organic Carbon
DOM	Dissolved Organic Matter
EC_{50}	Effective Concentration for 50% of Population
Em	Emission wavelength
Ex	Excitation wavelength
USEPA	United States Environmental Protection Agency
USGS	United States Geological Survey
FA	Fulvic Acid
FEEM	Fluorescence Excitation Emission Matrix
FI	Fluorescence Index
FQ	Fluorescence Quenching
HA	Humic Acid
ISE	Ion-Selective Electrode
Log K	Binding Constant
L_T	Binding Capacity
Ni	Nickel
$[Ni^{2+}]$	Concentration of free nickel ion
Ni-BLM	Nickel-specific BLM
NOM	Natural Organic Matter
$[Ni]_{Total}$	Total nickel concentration
OECD	Organisation for Economic Co-operation and Development
ppb	Parts per billion (µg/L)
ppm	Parts per million (mg/L)
SAC_{340}	Specific Absorbance Coefficient at Excitation = 340 nm
SIMPLISMA	SIMPLe to use Interactive Self-modeling Mixture Analysis
Trp	Tryptophan
Tyr	Tyrosine
WQC	Water Quality Criteria
WQG	Water Quality Guidelines

List of Tables

List of Equations

List of Figures

Table of Contents

1.0 Introduction

1.1 Nickel in the Environment

1.1.1 Sources in the Atmosphere and Water Systems

Nickel (Ni) is a ubiquitous element found in soil, air, and water, with an average crustal concentration of 75 µg/g (Poonkothai and Vijayavathi, 2012). Ni is the fifth most abundant element by weight (Cempel and Nikel, 2005), and has numerous deposits worldwide. Ni is number 28 on the periodic table, and is a group VIII element in the first row of transition metals (Poonkothai and Vijayavathi, 2012). It dissolves readily in aqueous systems and coordinates octahedrally in the form of $Ni[(H_20)_6]^{2+}$ (Chau and Kulikovsky-Cordeiro, 1995), and natural concentrations range from 0.2 to 0.7 µg/L in the open ocean and from 0.1 to 10 µg/L in fresh water (Wood *et al*., 2012). Coastal environments can have much higher values of 90 µg/L (Wells *et al*., 2000).

Large quantities of Ni are introduced into the environment every year from both natural and anthropogenic activities. Natural inputs include mineral erosion, volcanic eruptions, and forest fires (Cempel and Nikel, 2005). Ni inputs resulting from human activity include waste incineration, mining effluent, factory discharge, and surface run-off (Nriagu, 1990); these sources account for roughly 20% of anthropogenic Ni released each year, while the remaining 80% comes from coal combustion alone (Nriagu, 1990). Coastal Ni mining and smelting operations are located in Russia, Australia, New Caledonia and Indonesia, to name a few (Kuck, 2012).

1.1.2 Supply and Demand

Ni has great industrial appeal owing to its corrosion resistance, stability at elevated temperatures, malleability, and conductive characteristics (Wood *et al.*, 2012). The bulk of primary Ni is used in stainless steel production – approximately 60-68% (Kuck, 2012; Reck *et al*., 2008). Other uses include batteries (including nickel-cadmium batteries), wiring for electronics and machinery, and Ni-plating (Reck *et al*., 2008).

Ni is found in ores, the two most common being sulfide and laterite (Mudd, 2010). Sulfides result from hydrothermal processes and contain other elements, namely cobalt, copper, and some precious metals (Hoatson *et al*., 2006), while laterite ores are shallow deposits resulting from weathering of ultramafic rocks (Mudd, 2010). Approximately 60% of global Ni is reserved in laterite ores, but due to the complex nature of the laterite composition, they are costlier to refine than sulfide ores (Mudd, 2010). Until recently, sulfides provided the bulk of industrial Ni, accounting for up to 90% in the year 1950 (Oxley, 2016). Ni production has since increased tenfold, and to meet rising demands there has been more focus on laterite ore extraction (Mudd 2010); it is predicted that 72% of Ni will be sourced from laterites by 2022 (Oxley, 2016). Ni-laterite deposits are commonly located near the equator (Elias, 2002), with mining developments in New Caledonia, Indonesia, and the Philippines (USGS, 2012). Many of these mining sites are in coastal areas, creating a direct route for Ni to enter marine ecosystems.

The largest Ni deposit in the world is located in Sudbury, Ontario, and is sulfide-rich (Wood *et al*., 2012). Other Ni mines around the world include major sites in Russia, Australia, and others in Canada (USGS, 2012). Ten countries and territories account for nearly 70% of worldwide Ni production and manufacturing (Reck *et al*., 2008), with roughly 25% originating from the Sudbury deposit alone (Wood *et al*., 2012). In 2011, an all-time high of 2.05 Mt of mined nickel was produced around the world, and in the following year 1.66 Mt of primary nickel was used in industry, breaking the record for the third year in a row (USGS, 2012).

Prices of Ni have fluctuated over time as demands and global economy change and evolve. The years from 1970 to 1975 showed a slight rise in Ni prices, which had been relatively stable for a decade prior (USGS, 2010). In 1979, Ni contracts were made with the London Metal Exchange (LME) and it became the seventh most traded metal through the LME (USGS, 2010). Shortly after, however, the recession in 1981 caused a decrease in Ni demand, resulting in lower prices (USGS, 2010).

Between 1986 and 1988, Ni prices went from an all-time low to an all-time high when demands for stainless steel increased (USGS, 2010). Until the mid 1990's LME prices for Ni lessened because of an abundance of primary Ni production, but between 2001 and 2005 global Ni consumption increased steadily (~3.4% per year) (USGS, 2010). In the beginning of 2006, the price of Ni was $6.60 per pound, and in May 2007, it increased dramatically to $23.66 per pound (USGS, 2010).

In early 2016, global Ni prices were the lowest they had been in 13 years at $8,480 per metric ton ($3.81 per pound), owing to an oversupply of the metal, but the price rose to $10,262 per metric ton by October ($4.65 per pound; USGS, 2017); this was partially due to a 50% decrease in Ni production from the Philippines – the world's primary Ni ore producer – after failing to follow standard environmental procedures (USGS, 2017).

1.1.3 Pollution and Toxic Effects

Unfortunately, with elevated manufacturing and consumption rates comes increased environmental exposure to massive amounts of Ni every year. For example, areas surrounding the Sudbury mine are heavily contaminated: nearly 7,000 lakes are impacted and the Ni concentration ranges from 7 to 338 µg/L (Wood *et al.*, 2012). While evidence suggests that nickel is likely essential to fish, it can be toxic in certain forms and high concentrations (Wood *et al*., 2012). For example, EC_{50} values of 14 µg/L have been reported for *Evechinus chloroticus* – a common marine organism (Blewett *et al*., 2016).

Toxicity mechanisms for Ni are not as well-defined in seawater as they are for fresh water (Blewett *et al*., 2015). Although it is hypothesized that the difference in water chemistry between freshwater and saltwater should change the bioavailability of Ni, it is not understood what effect differences in physiology between marine and freshwater organisms might have on toxicity (Blewett and Leonard, 2017). Ni toxicity toward marine species is not the direct focus of this project, but it is recognized that there may be implications for toxicity mitigation by better understanding how Ni reacts in marine environments.

1.1.4 Recycling

Ni is an easy metal to recycle (Mudd, 2010) since it is typically used in large amounts and not in complex, difficult-to-separate mixtures (Reck and Graedel, 2012). Metals in general can theoretically be recycled an infinite number of times (Norgate *et al*., 2007), and recycling scrap Ni is much less harmful to the environment than is mining virgin Ni. As of 2007, global energy use in stainless steel production was reduced by 33% through recycling scrap, and CO_2 emissions lowered by 32% (Reck *et al*., 2008). Energy consumption and subsequent CO_2 release could theoretically be reduced by 67% and 70%, respectively, if austenitic stainless steel (35% Ni composition) were to be produced solely from scrap rather than from virgin-based sources (Reck *et al*., 2008).

While recycling is the obvious choice from an environmental perspective, it is costlier due to the collecting and sorting processes; therefore, mining new Ni is more economically viable (Graedel and Reck, 2012; Mudd, 2010). Recycling Ni may also not be as commonly practiced due to its abundance: the total estimated global reserve of Ni is 140 Tg, which is equivalent to 140,000,000,000 kg (Reck *et al.*., 2008), and a shortage is not expected in the foreseeable future.

Ni recycling is done in many countries, including the U.S., Taiwan, Germany, Canada, Russia, and the United Kingdom. In the United States, the largest source of scrap steel is automobiles, which are manufactured using austenitic steel (USGS, 2012). In 2016 the U.S. recycled approximately 43% of its total consumed Ni (USGS, 2017).

1.2 Nickel Speciation and Bioavailability

The most common form of nickel in natural waters within a normal pH range – between 5 and 9 – is the divalent ion, Ni^{2+} (Nriagu, 1980; Wood *et al*., 2012); this free ion is also the most toxic to aquatic organisms owing to it being the most bioavailable (Niyogi and Wood, 2004). The bioavailability of a chemical species is the portion available for biological uptake by organisms, and a chemical does not have

toxic effects on biota unless it is in a bioavailable form and at sufficiently high concentrations (CCME, 2007).

The range, or distribution, of an element in a system is termed speciation (Templeton *et al.*, 2000), and research suggests that there is a direct correlation between the speciation and bioavailability of metal ions (Campbell, 1995; Blewett and Leonard, 2017). The amount of Ni^{2+} ions present is dependent on several parameters: ambient pH, behavior of surrounding compounds in the water, and the tendency of the free metal ion to form complexes with organic and inorganic matter (CCME, 2008). Increasing complexation results in lower free ion concentrations, and with fewer Ni^{2+} ions comes reduced potential toxic effects toward aquatic organisms (Saar and Weber, 1980; Benedetti *et al.*, 1996).

Of the speciation-modifying factors, complexing ligands are specifically relevant (Di Toro *et al.*, 2001). There is a good understanding of inorganic materials and their interactions with nickel, for example established stability constants (Shadiq, 1989), but Ni-DOM complexation in general is not as clearly defined (Carson and Hansell, 2002).

1.3 Organic Matter

Natural organic matter (NOM) is a class of compounds that result from decomposed plant, animal, and microbial waste. The fraction of NOM able to pass through a 0.45 µm filter is operationally defined as dissolved organic matter (DOM), while the remainder is classified as particulate matter (Thurman, 1985). DOM is quantified by dissolved organic carbon (DOC), which composes approximately 50% of DOM (Wood *et al.,* 2011). DOM originates from both terrestrial sources (termed allochthonous) and within the water column (autochthonous) (Thurman, 1985).

Allochthonous DOM has a high percentage of aromatic rings and is dark in color (Wood *et al.*, 2011), whereas autochthonous DOM has relatively low aromaticity, is light in color and more protein-rich (McKnight *et al.*, 2001). Both allochthonous and autochthonous DOM are present in seawater, though amounts of autochthonous DOM are higher (Merdy *et al.*, 2011). DOM from both origins contains humic substances (HS) which are further categorized into humic acid (HA), fulvic acid (FA) and humin; FA accounts for 85% of marine HS, with HA as the remaining 15%; seawater HS concentrations range from 60 to 600 µg C/L, comprising up to 30% of oceanic DOC (Packham, 1964). Examples of theoretical molecular structures for HA and FA molecules are shown in Figures 1.1 and 1.2, respectively. HS are groups of large, heterogeneous polyfunctional hydrocarbons: FA tends to have molecular weights of <2,000 g/mol, and HA molecules are typically 2,000-5,000 g/mol (Thurman *et al.*, 1982).

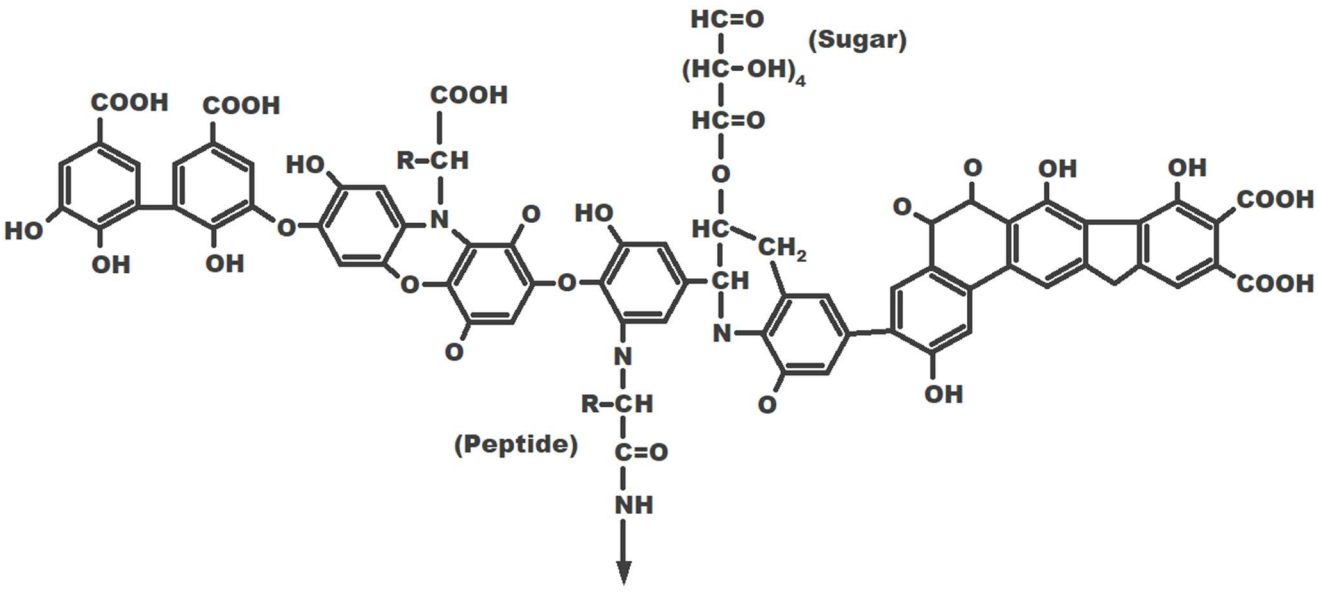

Figure 1.1: Representative humic acid molecule (Stevenson, 1982). This molecule has many aromatic moieties, as well as numerous functional groups (-COOH, -OH, -NH). The words in brackets indicate a sugar group (in this case, a carbohydrate) and a peptide.

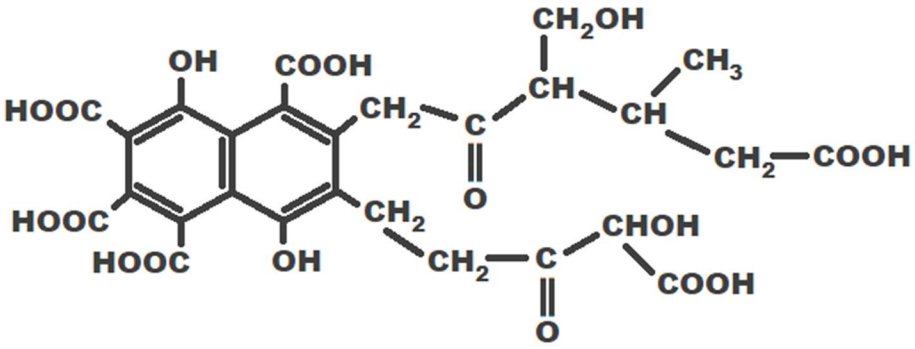

Figure 1.2: Representative fulvic acid molecule (Buffle, 1977).

Humin is insoluble throughout the pH range, and was not considered for the purposes of this project. HA molecules are soluble at pH > 2 and FA compounds are soluble throughout the pH range (Thurman, 1985). Both HA and FA have a variety of functional groups to which metal atoms can bind, including carboxyl-, amine-, ketone-, and phenol groups (examples in Figure 1.3) (Chon *et al*., 2013; Chen *et al.*, 2003). Ni has a higher affinity for sites containing nitrogen and oxygen than it does for sulfur-based functional groups (Wood *et al*., 2012).

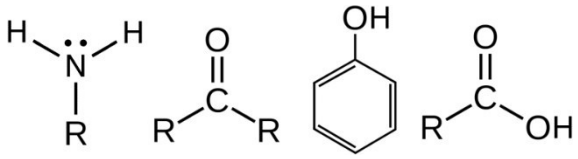

Figure 1.3: Generic functional groups, from left to right: a primary amine, a ketone, phenol, and a carboxylic acid.

DOM chemical composition is complex: there is a multiplicity of molecular forms of fulvic and humic acid, each with unquantified numbers of metal binding sites (Smith *et al*., 2002). Additionally, the range of chemical bonds between metals and these ligands - from predominantly electrostatic to predominantly covalent - is not well-defined for all metals, especially transition metals (Smith *et al.*, 2002).

1.4 Current Water Quality Guidelines and Criteria

In efforts to protect aquatic life, Water Quality Guidelines (WQG) and Water Quality Criteria (WQC) have been established in Canada and the United States, respectively. These guidelines and criteria

specify concentrations of Ni (in µg/L) that should not be exceeded; the Ni concentrations are based on toxicity assessment and evaluation tests, and the most current information available is used when established (CCME, 2007).

1.4.1 United States Criteria

The United States Environmental Protection Agency (USEPA) published ambient freshwater WQC for Ni in 1980 (USEPA, 1980). These included criteria for both acute and chronic Ni concentrations (in µg/L), using Equations 1 and 2, respectively (USEPA, 1980). Criteria for saltwater were also included in the 1980 document: Ni concentrations should not exceed 7.1 µg/L over a 24-hour average, and they should never exceed 140 µg/L. These values are expressed in terms of total recoverable metal (USEPA, 1980).

Acute [Ni] = exp {0.846 [ln(hardness)] + 2.255} **Equation 1**

Chronic [Ni] = exp {0.846 [ln(hardness)] + 0.0584} **Equation 2**

To quantify total recoverable metal, EPA criteria stipulate digestion of the sample with heated HCl and HNO_3 prior to quantitative analysis (USEPA, 2014). Dissolved metal concentrations are recognized as being the more accurate representation of the bioavailable fraction, but present criteria are still based on total recoverable concentrations (USEPA, 1993). To express them in terms of dissolved metal, the equations can be multiplied by a conversion factor (CF) (USEPA, 1993). The acute CF for saltwater is 0.990 (USEPA 2004). A chronic CF for saltwater has not been established, so the acute value is used for both acute and chronic Ni concentrations (USEPA 2004).

1.4.2 Canadian Guidelines

The first official Canadian Guidelines for the protection of aquatic life were released to the public by the Canadian Council of Resource and Environment Ministers - who later adopted the title 'Canadian Council of Ministers of the Environment' (CCME) - in 1987 (CCME, 2008). The most recent WQG are shown in Table 1.1.

Table 1.1: CCME Chronic Freshwater Quality Guidelines for the Protection of Aquatic Life (2017).

Water Hardness (in mg/L $CaCO_3$)	Maximum Ni Concentration (µg/L)
≤ 60	25
> 60 to ≤ 180	65 - 149*
> 180	150

* These values were determined by using Equation 3.

[Ni] = exp{0.76[ln(hardness)] + 1.06} **Equation 3**

To date, WQG are based solely on water hardness levels, in mg/L of $CaCO_3$ (CCME, 2007). Realistically, there are additional factors that influence how nickel behaves toward organisms, including pH, alkalinity, organic carbon, and the presence and concentration of other metals (CCME, 2003 & 2008). By only considering water hardness, WQG may be over- or under-protective depending on the site, since water chemistry varies between locations (CCME, 2003). All Canadian WQG, unless stated otherwise, pertain to total metal concentrations in unfiltered water (CCME, 2003 & 2007), though it is recognized that total metal concentrations are not an accurate measure of bioavailable fractions and that dissolved metal concentrations are more appropriate for understanding Ni toxicity (Campbell, 1995; Di Toro *et al*., 2001).

It should be noted that no Canadian WQG are in place for Ni in salt water (CCME, 2007). This issue can be mediated by developing a predictive model which incorporates the many metal speciation modifiers, that in turn affect the bioavailability - and ultimately toxicity - toward aquatic species; incorporating them will allow for more appropriate guidelines (CCME, 2007).

1.5 Biotic Ligand Model

The Biotic Ligand Model (BLM) is a computational tool used to predict metal toxicity toward different aquatic organisms. It does so by incorporating numerous biological and chemical variables:

organic and inorganic ligands in the water that can bind metal ions, sensitivity of different biota to the metals in question, and surrounding cations which compete for a binding site on the organism (the biotic ligand) (Niyogi and Wood, 2004). It has been demonstrated in some freshwater organisms, for example, that Ni toxicity depends on ambient Ni concentration, dissolved organic carbon, pH, hardness, salinity, and the unique physiology of the class of organism (Blewett and Leonard, 2017).

An example of a biotic ligand is gills on a fish (Di Toro *et al.*, 2001; Niyogi and Wood, 2004). Essential metal ions bind to these sites and cause different biological reactions, however non-essential ions can also interact with the biotic ligand and inhibit natural functions (Di Toro *et al.*, 2001). For example, Ni has been shown to interfere with magnesium receptors due to Mg^{2+} and Ni^{2+} having similar ionic radii (Lock *et al*., 2007). For fish and daphnids, Ni is a respiratory toxicant and an ion-exchange disruptor, respectively (Pane *et al*., 2003; Niyogi and Wood, 2004). Details on the modes of toxicity are outside the scope of this project, but multiple toxicity studies have been done (Blewett *et al*., 2017; Lock *et al*., 2007; Blewett and Leonard, 2017; Gissi *et al*., 2016; Tellis *et al*., 2014). A schematic overview of the BLM is pictured in Figure 1.4.

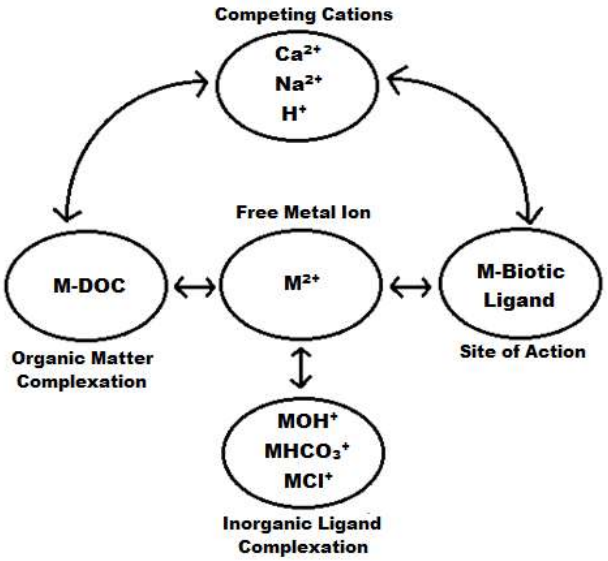

Figure 1.4: Simplified BLM Diagram (Di Toro *et al.*, 2001).

A BLM for copper has been implemented by Windward Environmental; the publicly available software allows analysis of between 1 and 1000 water samples simultaneously. Input variables of temperature, pH, DOC (in mg C/L), major cations, major anions, alkalinity, and sulfide concentrations are required for each sample (Windward, 2015).

This predictive model is a vision that has been in the making for many years (Di Toro *et al*., 2001). An acute Ni BLM is being researched for freshwater, although it is in the primary stage (Niyogi and Wood, 2004). At present, no marine-specific Ni BLM has been established, however progress is promising and a freshwater copper BLM has successfully been integrated in establishing WQC (USEPA, 2007; Tyle,2008).

1.6 Speciation Techniques

The BLM bases toxicity predictions on the bioavailable fraction (i.e., Ni^{2+}). Therefore, a speciation technique able to reliably quantify Ni^{2+}, particularly at environmentally-relevant concentrations, is necessary. This project considered two speciation techniques: potentiometry via an ion-selective electrode, and fluorescence spectroscopy.

1.6.1 Ion-selective Electrode

Popular speciation technique tools are ion-selective electrodes (ISEs). An ISE is comprised of a semi-permeable membrane that ideally allows migration of only one specific ion through the pores, an inner solution, and an inner reference electrode (Harris, 2010). Membranes used for metal ion detection, for example K^{+}, can be liquid-based, which refers to an organic polymer containing an ion exchanger (ionophore) (Harris, 2010). Ionophores are ligands with high affinity for the desired analyte (Harris, 2010).

The solution inside the ISE (inner solution) containing the analyte at a higher concentration than that in the sample being measured (Pretsch, 2002). The inner solution is in contact with the membrane, and the membrane is in contact with the sample. Due to the concentration difference on either side of the membrane, analyte ions will diffuse from the more concentrated inner solution, through the

membrane, to the less concentrated sample; this results in a charge imbalance which can be measured (Harris, 2010). The charge imbalance results in a potential that can be quantified as the difference between the internal reference electrode in the ISE, and an external reference electrode (Harris, 2010). The external reference electrode has a constant concentration; therefore, any changes in potential are a direct result of the analyte activity in the ISE (Harris, 2010). The potential is related to the analyte activity by the Nernst equation, shown below at equilibrium (Equation 4).

$$\mathbf{E^{\circ} = \frac{0.05916\ V}{n} log[A^{\pm n}]} \qquad \textbf{Equation 4}$$

Where E° is the standard reduction potential; n is the valence of the analyte; and A is the analyte. In the case of Ni^{2+}, n = 2, and the expected slope is therefore approximately 0.3 V, or 30 mV, per decade of concentration.

ISEs typically produce quick readings that are not influenced by color or turbidity, and samples measured by ISE do not require pretreatment; they also have a large detection range - generally on the order of 4 to 6 orders of magnitude (Harris, 2010). Unfortunately, no commercially available Ni-ISE exists (Doig and Liber, 2006; Saar and Weber, 1980); however, different groups have reported success with in-house Ni-ISEs (Abbaspour and Izadyar, 2001; Ganjali *et al*., 2002).

1.6.2 Fluorescence

Fluorescence is the phenomenon involving the release of a photon when electrons that are in an excited energy state return to the ground state (Valeur and Berberan-Santos, 2011). When radiation comes in contact with a compound and the amount of energy is exactly equal to the energy gap between the ground state and an excited state, the molecule absorbs this energy and the electrons get promoted to higher energy levels; after approximately 10^{-5} seconds, the electrons shift back to the lower energy state, emitting photons (Valeur and Berberan-Santos, 2011).

Fluorescence spectroscopy is an established technique for studying qualitative properties of organic compounds (Hudson *et al*., 2007) because organic matter - and its dissolved fraction - fluoresces due to high levels of aromaticity (Lakowicz, 2006). This technique allows for differentiation of fluorescent components within a sample based on the wavelengths where fluorescence intensity is measured, and can serve as an indicator of DOM source (Merdy *et al*., 2012). There are two main types of fluorophores when considering DOM: "humic-like," which emit energy between wavelengths of 400 and 500 nm (Coble, 1996), and "protein-like," which emit between 300 and 380 nm (Birdwell and Engel, 2011; Chen *et al*., 2003).

Benefits of fluorescence spectroscopy include small sample volume requirements, little- to no sample pretreatment, and highly sensitive results; it is also non-destructive, allowing for the sample to be used again for further analysis (Birdwell and Valsaraj, 2010). Unfortunately, a limitation of fluorescence spectroscopy is its inability to detect non-fluorescent ligands (Cabaniss, 1992; Tait *et al*., 2016); thus, using fluorescence to estimate log K and L_T values for metals may not be representative. However, a study comparing ISE measurements with fluorescence data for copper yielded results that were all within a 95% confidence interval of one another, suggesting that fluorescence spectroscopy can provide sufficient information on speciation of metals (Tait *et al*., 2016).

Different types of fluorescence measurements were performed during this project, namely fluorescence excitation emission matrices (FEEMs) and synchronous scans. A FEEM is a 3-dimensional spectrum resulting from scanning the sample over a range of both excitation (Ex) and emission (Em) wavelengths. Merdy *et al*. (2011) described FEEMs as 'fingerprints' since the technique can differentiate between whether the organic matter is derived from bacteria, or if it is terrestrial in origin. FEEMs provide both qualitative and quantitative information (Huguet *et al*., 2009). An example FEEM is shown in Figure 1.5.

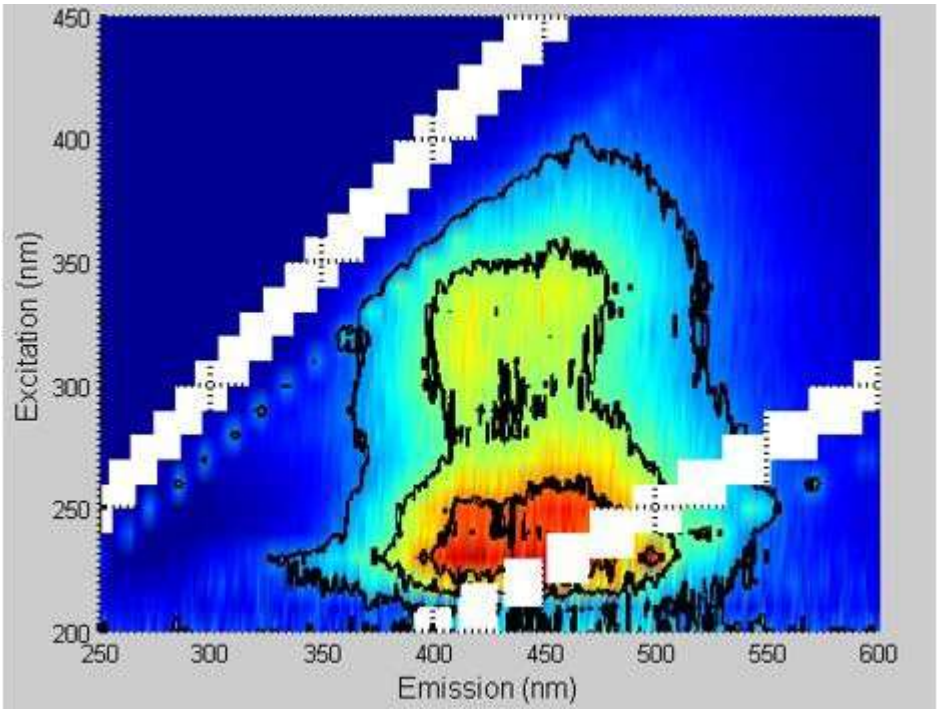

Figure 1.5: Example FEEM of DOM, taken from present study; x-axis is emission wavelength (nm) and y-axis is excitation wavelength (nm). The different colours represent the fluorescence intensity in arbitrary units (au), ranging from dark blue (least intense) to red (most intense).

Synchronous scans are a 2-dimensional spectrum 'slice' within a FEEM. These scans span a range of Ex and Em wavelengths (Hudson *et al*., 2007) and can monitor changes in fluorescence intensity during titrations of DOM with metals; these scans are useful because they provide the same information as a FEEM, but take only a fraction of the time to scan.

Both log K and L_T values can be determined from the resulting data by using the famous Ryan-Weber equation (Equation 5) (Ryan and Weber, 1982). Unlike DOM, most metal ions do not fluoresce. Saar and Weber (1980) reported fluorescence quenching of soil fulvic acid when titrated with Ni^{2+}, and highlighted that fluorescence spectroscopy can provide valuable information on metal ion complexes for species such as Ni^{2+} where no commercial ISE exists. More recent studies have also reported similar results for copper interactions (Smith and Kramer, 2000; Chen *et al*., 2013), and for mercury (Chen *et al*., 2013).

The Ryan-Weber equation allows both the complexing capacity and the stability constant to be solved for through nonlinear regression; the equation is as follows:

$$\boldsymbol{I = (\frac{I_{ML}-100}{2KC_L})\,[(KC_L + KC_M + 1) - \sqrt{(KC_L + KC_M + 1)^2 - 4K^2C_LC_M}\,] + 100} \qquad \textbf{Equation 5}$$

Where I is the measured fluorescence intensity; I_{ML} is the fluorescence intensity value that will no longer decrease even with further addition of metal; K is the stability constant; C_L is the complexing capacity; and C_M is the total metal ion added (Ryan and Weber, 1982). The stability constant is a measure of how strongly the metal ion associates with the ligand, and is usually determined by measuring free metal ions in a solution where concentrations of both the ligand and total metal are known (Saar and Weber, 1980). However, in instances where free ion concentration is not easily quantified, measuring the amount of complexed and/or uncomplexed ligand can serve as a way to solve for the stability constant Equation 6 (Saar and Weber, 1980; Harris, 2010).

$$\mathbf{K = \frac{[ML]}{([M][L])}} \qquad \textbf{Equation 6}$$

Where [ML] is the concentration of metal-ligand complex, and [M] and [L] are the concentrations of unbound metal and unbound ligand, respectively. Another piece of information that can be extracted from fluorescence data sets is fluorescence index (FI). FI is the ratio of fluorescence intensities occurring at emission wavelengths 450 nm and 500 nm after an excitation wavelength of 370 nm (Ex = 370 nm, Em = 450/500 nm) (McKnight *et al*., 2001). Values up to 1.4 signify that the DOM is allochthonous, and values of 1.9 or greater signify proteinaceous DOM; therefore, FI can indicate the source of DOM (Birdwell and Engel, 2010).

1.7 Research Objectives and Significance

The purpose of this study was to identify an effective speciation measurement technique for Ni in seawater, and to analyze the interactions of Ni with DOM in a variety of real samples. It was

hypothesized that if the idea behind the BLM is correct, Ni^{2+} concentrations at EC_{50} levels will be the same for an organism, regardless of sample composition. Cooper *et al*. (2014) made this connection for copper in saltwater, and thus validated BLM applications for marine copper.

In other words, the BLM theorises that the amount of Ni^{2+} accumulated at the biotic ligand at the EC_{50} level is the same for organisms of the same species. DOM quality and other variables affect Ni^{2+} binding such that the amount of Ni required to reach the same concentration at the biotic ligand is different between water samples, but that ultimately the same concentration of Ni^{2+} is present each time. Therefore, this study aimed to reliably measure [Ni^{2+}] in seawater by using fluorescence and ISE techniques.

Chapter 2: Materials and Methods

2.1 Sample Preparation

2.1.1 East Coast Samples

Water samples used for the purposes of this project were collected at various coastal sites in the northeastern United States, hereafter referred to as the East Coast samples (for map, see Appendix F1). There were three collection trips: July 2015, October 2015, and June 2016. Originally there were ten sampling sites (Table 2.1) and all water samples collected were used for blue mussel and purple sea urchin embryo toxicity studies (Blewett *et al.*, 2017). The test results indicated which samples were protective against Ni toxicity relative to the control (artificial seawater, ASW); based on this information, only certain sites were revisited during the second and third collections.

Table 2.1: East Coast sampling site information.

Sample	Name	Site & Description	GPS Coordinates
0	KMS	Artificial seawater: Kent Marine Salt in MilliQ water.	--
1	SVP	Seaview Park: Terrestrial inputs.	41° 45' 40.6'' 071° 23' 11.5''
2	BTP	Barbara Tufts Playground: Sewage inputs.	41° 39' 30.9'' 071° 26' 51.7''
3	PCA	Perry Creek Access: Salt marsh.	41° 21' 49.4'' 071°37' 36.1''
4	BBP	Beebe Pond: Mud flat.	41° 20' 14.4'' 071° 59' 29.7''
5	ELM	80 Elm Street: Ocean coast with abundance of seaweed.	41° 19' 46.4'' 071° 59' 26.8''
6	GCT	Guilford Land Conservation: Tidal salt marsh, muddy.	41° 17' 04.8'' 072° 41' 14.3''
7	CCHT	Audubon Coastal Centre (high tide): Salt marsh, many plants.	41° 10' 34.7'' 073° 06' 04.2''
8	IR	Indian River: Terrestrial inputs to salt marsh.	41°13' 39.9'' 073° 02' 13.8''
9	WB	Walnut Beach: Open sandy beach, no large vegetation.	41° 11' 49.6'' 073° 04' 28.5''
10	CCLT	Audubon Coastal Centre (low tide): Site 7, but at low tide.	41° 10' 34.7'' 073° 06' 04.2''

All samples were collected in new, 1 L Nalgene bottles that were rinsed with sample prior to filling. During each collection, measures were taken to reduce exposure of the samplesto air by capping bottles while submerged. Sample containers were transported in ice-filled coolers. Once in the lab, all samples

were brought to full-strength seawater salinity (~32 mg/L) through the addition of Kent Marine Reef Salt Mix (KMS; purchased at Big Al's Aquarium in Kitchener, ON). Salinities were measured with a YSI salinity probe (Professional Plus), and ambient salinities are shown in Table 2.2. Samples from the first two collections were then filtered through 0.45 µm membranes (Whatman™ cellulose nitrate membrane filters) to remove particulate matter. Third collection samples were filtered on-site with a 0.3 µm membrane (Rainfresh® ceramic cartridge with activated carbon core, purchased at Canadian Tire) and were not filtered a second time after adding salt. All samples from each sampling trip were stored at 4° C in the dark prior to titrations and toxicity testing, and while not in use.

Table 2.2: Ambient salinities of East Coast samples (before addition of Kent Marine Salt).

Sample	Salinity (ppt)	Sample	Salinity (ppt)
SVP	5.5	GCT	11.63
BTP	13.07	CCHT	16.76
PCA	27.11	IR	24.05
BBP	25.52	WB	24.38
ELM	27.46	CCLT	12.81

2.1.2 Other Samples

Several other samples were used as side studies in this project, including several samples of protein skimmer waste from a local aquarium store (Living Aquarium in Cambridge, ON), and a grab sample from Belize (GPS coordinates: 17° 13' 12.4'', 87° 35 '36.9''). The salinities of all samples were brought to a final salinity of ~32 mg/L by adding Kent Marine Salt while constantly stirring. Prior to experimentation, the samples were filtered through a clean, 0.45 µm polyethersulfone membrane (25 mm syringe filter, VWR International, USA). FEEMs were run of all samples, but only the Belize and 'Small Solid' protein samples were titrated.

2.2 Ion-selective Electrode

2.2.1 Design and Assembly

An electrode kit was purchased (Electrode Body ISE 45137, Fluka Analytical, distributed by Sigma-Aldrich Production GmbH), which included an inner reference electrode and an outer casing to hold the filling solution and membrane inside. A diagram is shown in Figure 2.1. Two membranes were prepared, each using a different ionophore: dithizone (1,5-diphenylthiocarbazone) and BBTC (benzylbis(thiosemi-carbazone)). Chemical structures of dithizone and BBTC are shown in Figures 2.2 and 2.3, respectively.

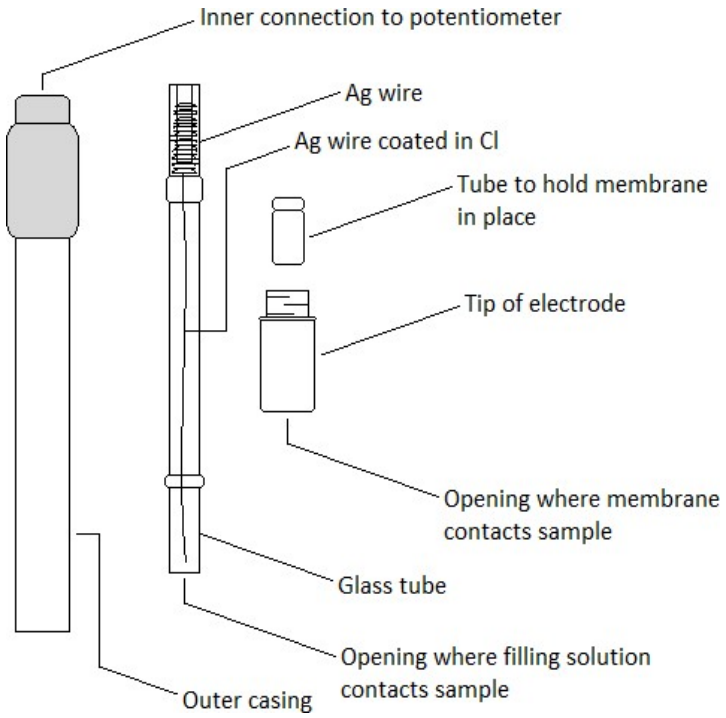

Figure 2.1: Diagram of electrode kit (left).

The procedure by Abbaspour and Izadyar (2001) was followed for the dithizone membrane, the only change being that the membrane mixture was allowed to dry prior to assembling the ISE. This was done by pouring the mixture into a ring on a glass surface for 48 hours. Once dry, a small, circular membrane was cut from the master membrane and placed into the tip of the electrode. The filling solution of 0.05 M $Ni(NO_3)_2$ and 0.05 M KNO_3 was prepared, and after assembly the electrode was placed in a conditioning solution of 0.05 M Ni standard for 24 hours (Abbaspour and Izadyar, 2001).

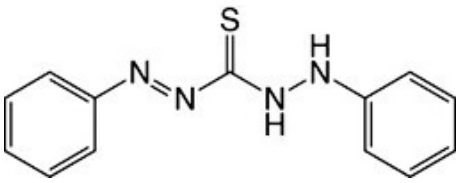

Figure 2.2: Chemical structure of dithizone (1,5-diphenylthiocarbazone).

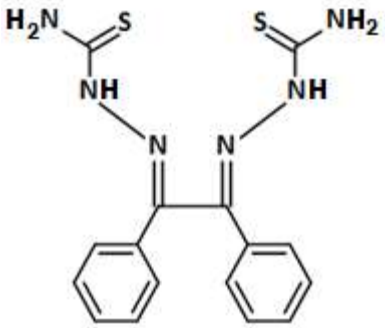

Figure 2.3: Chemical structure of BBTC (benzylbis(thiosemi-carbazone)).

A membrane using the BBTC ionophore was also prepared (Ganjali *et al.*, 2002). As with preparation of the dithizone membrane, the BBTC mixture was poured into a glass ring to dry, and then the dried membrane was cut and placed into the electrode body. The filling solutions were varied to optimize the electrode's response, and the conditioning solution was 0.01 M $Ni(NO_3)_2$ for 24 hours prior to calibration. Both membranes used polyvinyl chloride (PVC) as the polymer matrix (Abbaspour and Izadyar, 2001; Ganjali *et al.*, 2002); PVC is a hydrophobic compound that holds the ionophore in place (Harris, 2010).

2.2.2 Calibration

Once conditioned, each electrode was calibrated. Starting with a solution of 1.0×10^{-6} M $Ni(NO_3)_2$, small volumes of $Ni(NO_3)_2$ were added after the response stabilized (≤ ±0.5 mV over 5 minutes). The Ni ISE was connected to a potentiometer (Tanager Scientific Systems Inc., Model 9501, Ancaster, ON), as was an external Ag/AgCl reference electrode (Orion™ 900200 Sure-Flow™ Reference Half-Cell Electrode, Thermo Fisher Scientific, Beverly, MA, USA). The concentration range of calibration solutions was 5.0×10^{-6} M to 1.0×10^{-2} M, and potentiometric measurements were recorded every 2 minutes. Solutions were continuously stirred (using a stir plate and magnetic stir bar) for the duration of the calibration, and the pH was periodically measured using a Beckman Coulter pH meter (Model pHi 570 Benchtop). The Ni ISE

was removed from solution while the pH was measured due to interference between the two electrodes. All calibration data was plotted as potential versus added [Ni] as per the Nernst equation (Equation 4 in Section 1.6.1) to determine the slope of the calibration curve.

2.3 Fluorescence

2.3.1 Fluorescence Excitation-Emission Matrices

Fluorescence excitation-emission matrices (FEEMs) were scanned for each DOM sample to determine the optimal wavelength range 'slice' at which to perform fluorescence-monitored titrations. The same parameters were used each time (Table 2.3), except for third collection samples which used PMT detector settings of 1000 V to enhance low-intensity signals. All scans were done with a Varian Cary Eclipse Fluorescence Spectrophotometer (Agilent Technologies, Santa Clara, CA), and the samples were held in a 1 cm pathlength quartz cuvette (Type 3-Q-10, Lightpath Optical (UK) Ltd.). FEEMs were plotted in MATLAB (MathWorks, Natick, MA, USA) using an in-house Matlab code (see Appendix C1).

Table 2.3: Fluorescence spectrophotometer settings for FEEMs.

Parameter	Settings
Excitation range (nm)	200 – 450
Emission range (nm)	250 – 600
Slit width (nm)	5
3D mode	On
Excitation increment (nm)	10
Scan speed (nm/min)	600
PMT detector (V)	800

2.3.2 Fluorescence Monitoring

Samples from the second and third collections were scanned every few days with a portable fluorimeter (SMF4 Fluorimeter, Safety Training Systems Ltd.) as a quick means of monitoring composition changes over time. While not an extensive technique, the fluorimeter is a convenient, easy-to-use tool that gives a reading within a matter of seconds. A 1 cm pathlength quartz cuvette was used, and before each sample it was thoroughly rinsed with MilliQ. The sensitivity of the fluorimeter was set to 'high' and five scans were taken of each sample.

2.3.3 Fluorescence Quenching Titrations

Fluorescence quenching (FQ) titrations were also performed on the Varian Cary Eclipse Fluorescence Spectrophotometer, with a 1 cm pathlength flow-through quartz cuvette (Starna Cells Inc., Atascadero, CA). Polyvinyl chloride tubing (Gilson, 2.79 mm I.D.) was connected to the cuvette, and a peristaltic pump (Gilson Minipuls 2, France) was used to circulate the sample from a beaker to the cuvette. Before and after each titration, the setup was thoroughly rinsed with MilliQ water, and a FEEM of MilliQ was scanned before titrating to ensure that the tubing and cuvette were clean and free of contamination. If contamination was suspected - and after 3-4 titrations regardless - an acidified rinse was circulated through the system, followed by a thorough MilliQ rinse. The acidified rinse was made by adding several drops of ACS grade HCl (EMD Chemicals, Gibstown, NJ, USA) to MilliQ until a pH of ~2 was achieved.

Nickel titrant was prepared by dissolving $NiSO_4 \bullet 6H_2O$ crystals (Fisher Chemical, Certified ACS Grade) in MilliQ water. All samples were brought to - and maintained at - a pH of 8.00 ± 0.05 with 1.0 M and 0.1 M samples of both NaOH (J.T. Baker) and HNO_3 (Fisher Scientific). Samples were stirred continuously during the titrations, and the titrant was added in increments until a final concentration of approximately 530 ppb Ni was reached in the sample. After each addition, the sample was stirred for 15 minutes before synchronous scans were done in triplicate (see Appendix C2).

2.4 Sample Analysis

2.4.1 Graphite Furnace Atomic Absorption Spectrometry

After the FQ titrations, the Ni in the samples was measured with a graphite furnace atomic absorption spectrometer (PinAAcle 900T AA, Perkin Elmer, Waltham, MA). For referencing purposes, ASW was prepared with a mixture of salts in MilliQ water, as per specifications by the Organisation for Economic Co-operation and Development (OECD); the recipe is shown in Table 2.4. This OECD ASW was used to in the calibration solutions, along with certified Ni standard (Ultra Scientific, Kingstown, RI, USA). All calibration solutions and samples were acidified with 2% trace metal grade HNO_3 (Omni*Trace* Ultra™, Millipore Sigma, Darmstadt, Germany).

Table 2.4: OECD recipe for artificial seawater.

Salt	Mass (for 1 L ASW)	Supplier
NaF	3 mg	Fisher Chemicals
$SrCl_2 \cdot 6H_2O$	20 mg	Fisher Chemicals
H_3BO_3	30 mg	Sigma-Aldrich Corp.
KBr	100 mg	BDH
KCl	700 mg	Sigma-Aldrich Corp.
$CaCl_2 \cdot 2H_2O$	1.47 g	Fisher Chemicals
Na_2SO_4	4.0 g	Fluka Analytical, Sigma-Aldrich Corp.
$MgCl_2 \cdot 6H_2O$	10.78 g	Sigma-Aldrich Corp.
NaCl	23.5 g	Anachemia Canada Co.
$Na_2SiO_3 \cdot 9H_2O$	20 mg	Fisher Chemicals
$NaHCO_3$	200 mg	EMD Chemicals

2.4.2 Total Organic Carbon Analysis

All samples were measured on a Carbon Analyzer (TOC-L_{CPH} Carbon and Nitrogen Analyzer, Shimadzu Corp., Kyoto, Japan) to quantify both the total and dissolved organic carbon. Samples were passed through 0.45 µm syringe filter membranes if DOC was being measured; otherwise they were left unfiltered to determine TOC. If highly coloured, the samples were diluted with MilliQ. All samples were brought to a pH of 2-3 with ACS grade HCl prior to analysis to help purge the dissolved inorganic carbon (EMD Chemicals, Gibstown, NJ, USA).

2.4.3 Computational (Matlab) Analysis

Raw titration data from each sample were entered into Matlab, and a SIMPLISMA ("SIMPLe to use Interactive Self-modeling Mixture Analysis") code was applied to solve for relative fluorophore concentrations within each sample (see Appendix C3). The data needed for this was the range of emission wavelengths, as well as the fluorescence intensity throughout this range after each Ni addition. Parameters were adjusted to 'zoom in' to the data where the largest change in fluorescence intensity occurred. SIMPLISMA is commended for making it straightforward for the user to recognize poor spectral resolution (Windig *et al*., 1992). This code was written to account for two fluorophores, although if the resolved spectra overlapped, it was assumed that only one fluorescent component was present. More than two components gave uninterpretable spectroscopic results.

The SIMPLISMA results were entered into a Matlab code (see Appendix C4) and fitted to the Ryan-Weber equation (Equation 5). Values for 'logK,' 'logLT,' and '%inefficiency' were adjusted in the code to create a manual best fit and to minimize potential error. Running this code yielded log K, log L_T, and the percent inefficiency - the factor by which the fluorescence intensity has changed (ie. if quenching occurred, this value will be <1.0; if enhancement occurred, it will be >1.0). This procedure was followed from Tait *et al*., 2016.

$$\boldsymbol{I = \left(\frac{I_{ML} - 100}{2KC_L}\right)\left[(KC_L + KC_M + 1) - \sqrt{(KC_L + KC_M + 1)^2 - 4K^2C_LC_M}\right] + 100} \qquad \textbf{Equation 5}$$

The last step of computational analysis was quantifying free Ni^{2+} concentrations at EC_{50} levels in some of the samples from toxicity tests performed by Blewett *et al.* (2017). This was done with Monte Carlo analysis (see Appendix C5), and inputting values from the Ryan-Weber analysis (averages and standard deviations of both log K and log L_T) as well as the total Ni concentrations at EC_{50} values for each sample. Monte Carlo analysis is a probability simulation that varies input parameters according to their standard deviations, and runs simulations hundreds to thousands of times with different variations; it can estimate uncertainty based on the distribution of results (RiskAMP, 2017).

For both the Ryan-Weber fitting and the Monte Carlo analysis, an inorganic complexation model was assumed. A tableau of Ni and probable inorganic chemical species is shown in Figure 2.4. Each column corresponds to the element at the top, and the log K values were obtained from the National Institute of Standards and Technology (NIST) for the respective compounds in seawater ionic strength (Martell and Smith, 2004).

H^+	Ni^{2+}	CO_3^{2-}	SO_4^{2-}	Cl^-	L1	L2	log K	Species
1	0	0	0	0	0	0	0	H
0	1	0	0	0	0	0	0	Ni^{2+}
0	0	1	0	0	0	0	0	CO_3^{2-}
0	0	0	1	0	0	0	0	SO_4^{2-}
0	0	0	0	1	0	0	0	Cl^-
0	0	0	0	0	1	0	0	L1
0	0	0	0	0	0	1	0	L2
-1	0	0	0	0	0	0	-14	OH
1	0	1	0	0	0	0	9.53	HCO_3^-
2	0	1	0	0	0	0	15.5	H_2CO_3
1	0	0	1	0	0	0	0.7197	HSO_4^-
-1	1	0	0	0	0	0	-10.02	$NiOH^+$
0	1	1	0	0	0	0	3.57	$NiCO_3$
0	1	0	1	0	0	0	0.7737	$NiSO_4$
1	1	1	0	0	0	0	11.12	$NiHCO_3^+$
0	1	0	0	1	0	0	-0.46	$NiCl^+$
0	1	0	0	0	1	0	K(1)	NiL1
0	1	0	0	0	0	1	K(2)	NiL2

Figure 2.4: Tableau of inorganic Ni complexes used in Matlab analyses.

Chapter 3: Results and Discussion

3.1 Ion-Selective Electrode

3.1.1 Dithizone (1,5-diphenylthiocarbazone)

The first ionophore used was 1,5-diphenylthiocarbazone (Dithizone) and was expected to have a response of 29.1 mV/decade over a $Ni(NO_3)_2$ concentration range of 5.0×10^{-6} M to 1.0×10^{-2} M (Abbaspour and Izadyar, 2001). Several calibration conditions were tested (Table 3.1), however the results were either unreliable or not reproducible – slopes ranged from 0.1533 to 32.879 mV/decade, and the ISEs tended to respond differently from one calibration to the next. For example, Test 8 conditions gave a slope of -3.2261 mV/decade when repeated in Test 12.

Table 3.1: Summary of calibration tests with Dithizone membrane.

Test	Filling Solution	Calibrating Solutions (5.0×10^{-6} M – 1.0×10^{-2} M)	Slope (mV/decade)	R^2
0	0.05 M $Ni(NO_3)_2$ + 0.05 M KNO_3	$Ni(NO_3)_2$	29.1 (Abbaspour & Izadyar, 2001)	0.999
1	0.05 M Ni std. + 0.05 M KNO_3	Ni std. *	32.879	0.995
2	0.05 M Ni std. + 0.05 M KNO_3	$NiSO_4$ (in ASW) (1.0×10^{-9} M – 1.0×10^{-4} M)	0.1533	0.005
3	0.05 M Ni std. + 0.05 M KNO_3	$NiSO_4$ (in ASW) (1.0×10^{-9} M – 1.0×10^{-4} M)	1.7411	0.248
4	0.05 M $NiSO_4$ + 0.1 M NaCl	Ni std. in 0.01 M acetic acid **	-8.5086	0.640
5	0.05 M $NiSO_4$ + 0.1 M NaCl	$NiSO_4$	30.541	0.783
6	0.05 M $Ni(NO_3)_2$	Ni std.	11.498	0.909

	+ 0.05 M KNO_3			
7	0.05 M $Ni(NO_3)_2$ + 0.05 M KNO_3	$Ni(NO_3)_2$	-23.893	0.996
8	0.05 M $Ni(NO_3)_2$ + 0.05 M KNO_3	$NiSO_4$	7.6059	0.9548
9	0.05 M $Ni(NO_3)_2$ + 0.05 M KCl	$NiSO_4$	8.9761	0.846
10	0.05 M $Ni(NO_3)_2$ + 0.05 M KNO_3 + 0.05 M EDTA	$NiSO_4$	6.5167	0.9885
11	0.05 M $Ni(NO_3)_2$ + 0.05 M KCl + 0.05 M EDTA	$NiSO_4$	-4.6833	0.8969
12	0.05 M $Ni(NO_3)_2$ + 0.05 M KNO_3	$NiSO_4$	-3.2261	0.7365
13	0.05 M $Ni(NO_3)_2$ + 0.05 M KNO_3 + 0.05 M EDTA	$NiSO_4$	0.7888	0.6333
*Ni std. is a certified Ni standard (Ultra Scientific, Kingstown, RI, USA) **pH was adjusted to 4 with 0.1 M NaOH				

Of all trials, the calibration that yielded the most Nernstian result was Test 1 with a slope of 32.879 mV/decade. However, the same electrode showed no response in ASW (Tests 2 and 3), likely due to calcium and magnesium accumulation at the ISE surface which would prevent further change in response. Therefore, no sample titrations were performed with Dithizone-based membranes.

3.1.2 BBTC (Benzylbis(thiosemicarbazone))

Results for the Ni ISE with the benzylbis(thiosemicarbazone) (BBTC) ionophore were more promising. Ganjali *et al*. (2002) reported slopes of 29.0 ± 0.5 mV/decade over a $Ni(NO_3)_2$ concentration

range of 1.0 x 10^{-7} M to 1.0 x 10^{-2} M. While values from the present study were not Nernstian (Table 3.2), the electrode was responsive and the results were reasonable (i.e. no negative slopes and consistently high R^2 values).

Table 3.2: Summary of calibration tests with BBTC membrane; all tests were performed with the same filling solution (0.05 M $Ni(NO_3)_2$ + 0.05 M KCl + 0.05 M EDTA) and calibrating solutions (1.0 x 10^{-6} M – 1.0 x 10^{-2} M $NiSO_4$).

Test	Slope (mV/decade)	R^2	Test	Slope (mV/decade)	R^2
1	22.732	0.9982	10	8.5698	0.9757
2	20.698	0.9989	11	7.3125	0.9897
3	10.881	0.9847	12	11.833	0.9897
4	9.2094	0.9707	13	11.155	0.9236
5	8.9263	0.9972	14	12.169	0.9855
6	8.2007	0.9974	15	10.653	0.9642
7	8.2329	0.9916	16	14.709	0.9917
8	7.1545	0.9724	17	16.864	0.9994
9	7.5677	0.9838	18	18.068	0.9946

Samples of freshwater DOC were titrated including two samples from the International Humic Substances Society (IHSS), an Amazon grab sample, and an Amazon concentrate. The Amazon sample was a composite of surface waters, collected at the same time as the study by Johannsson *et al.* (2017), and concentration of the sample was achieved through reverse osmosis (RO) (Duarte *et al.*, 2016). Figure 3.1 shows a 1:1 dashed line where $[Ni]_{Total}$ is equal to $[Ni^{2+}]$, and everything below this line is indicative of Ni binding. Luther Marsh samples displayed very little to no Ni^{2+} binding, while Suwannee River samples showed substantial binding in comparison. Amazon samples fell in the middle, suggesting moderate

binding.

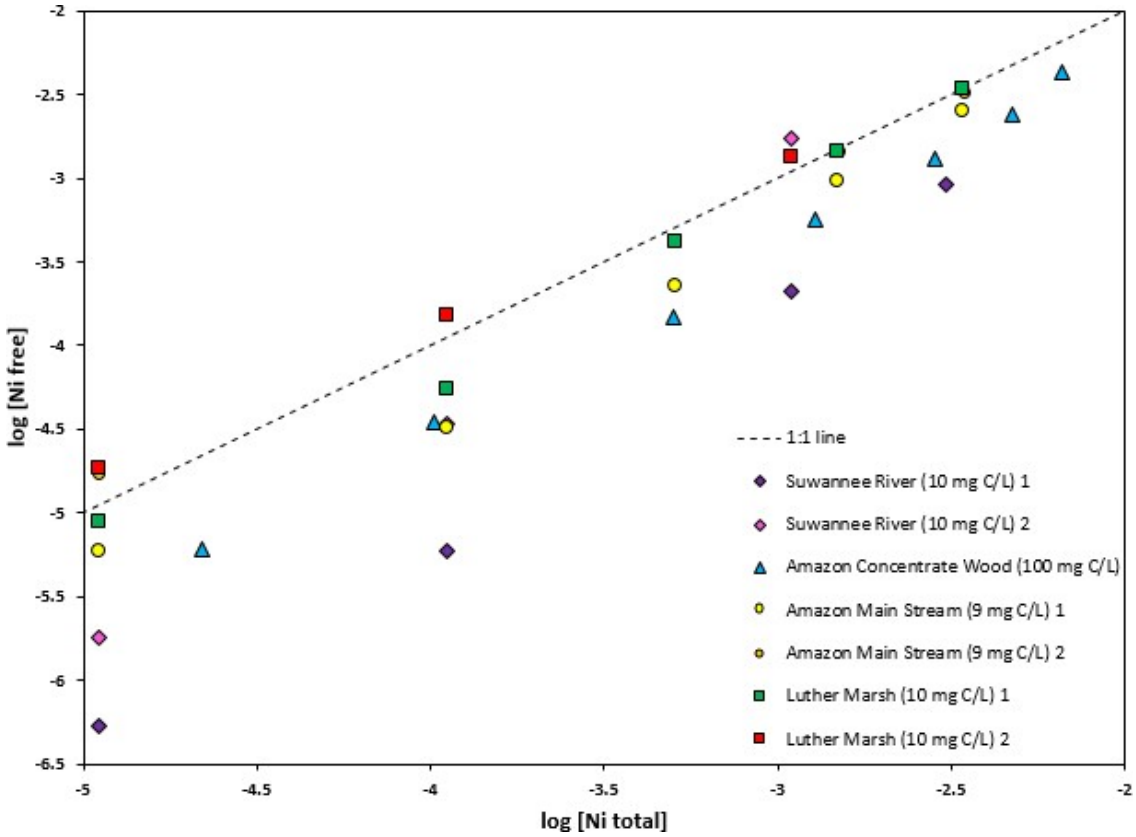

Figure 3.1: All freshwater Ni-DOC titrations done with BBTC membrane; x-axis is log of $[Ni]_{Total}$ added, and y-axis is log of $[Ni^{2+}]$. DOC concentration within each sample is included in the legend in brackets.

While the Ni-ISE showed potential for freshwater, no response was detected during titrations in salt water (an example trial is shown in Figure 3.2); this is likely owing to cation competition. High concentrations of calcium ions (Ca^{2+}) and magnesium ions (Mg^{2+}) in sea water can interfere with Ni^{2+} uptake. Therefore, focus toward identifying a reliable speciation technique was shifted to fluorescence.

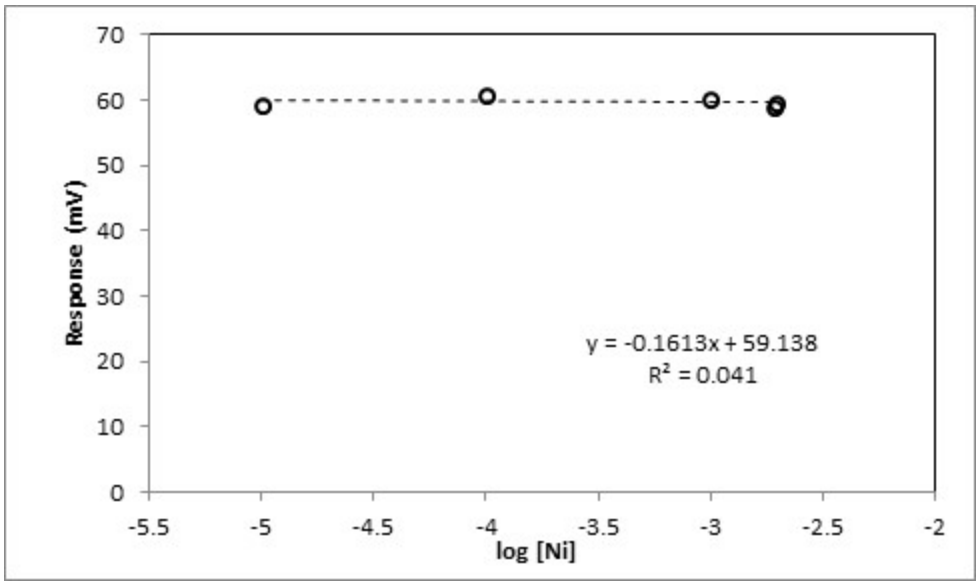

Figure 3.2: ASW calibration with BBTC membrane, showing no response to Ni^{2+}; x-axis is log [Ni^{2+}], and y-axis is response in mV.

3.2 Fluorescence

3.2.1 Fluorescence Excitation-Emission Matrices

FEEMs were scanned for each sample from every collection. Figure 3.3 shows FEEMs for sites SVP, BTP, BBP, ELM, CCHT, and CCLT each time they were collected (see Table 2.1 for sample details). Figure 3.4 shows FEEMs for Belize and 'Small Solid' samples. For all other sample FEEMs, refer to Appendix F2.

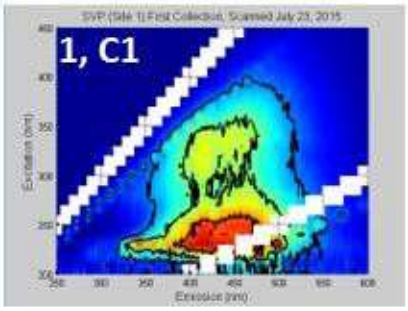
1, C1

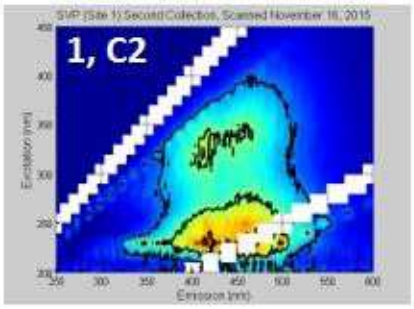
1, C2

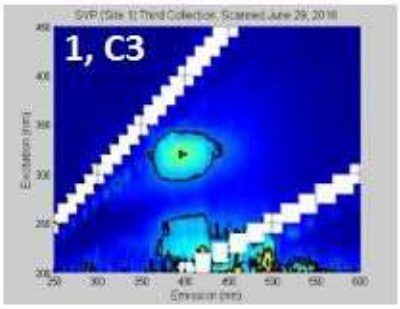
1, C3

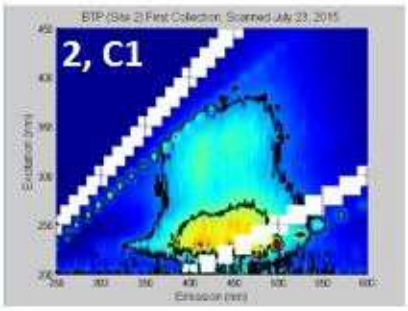
2, C1

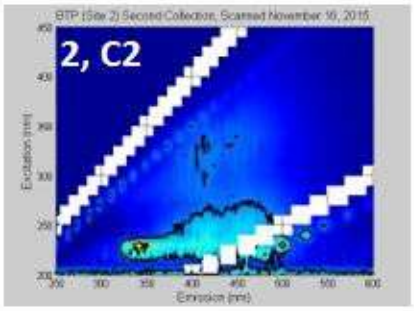
2, C2

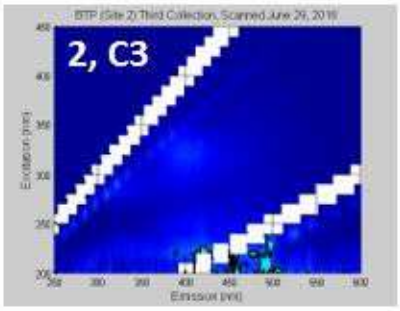
2, C3

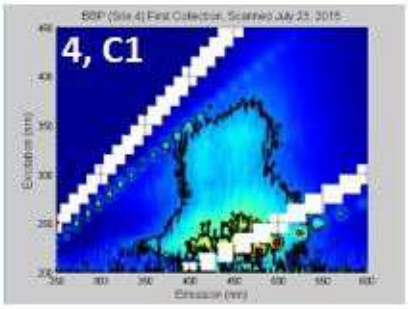
4, C1

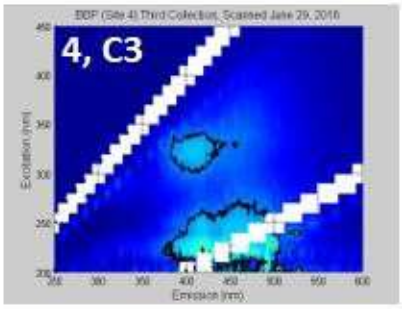
4, C3

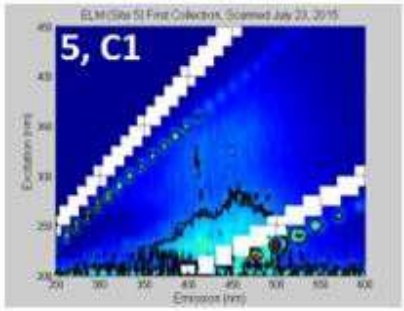
5, C1

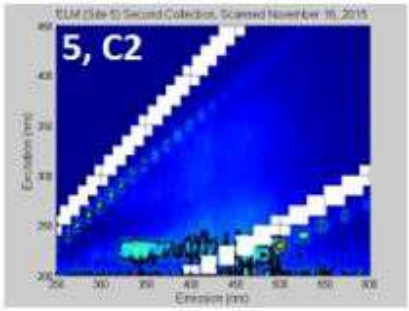
5, C2

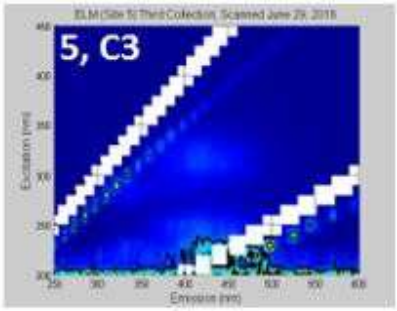
5, C3

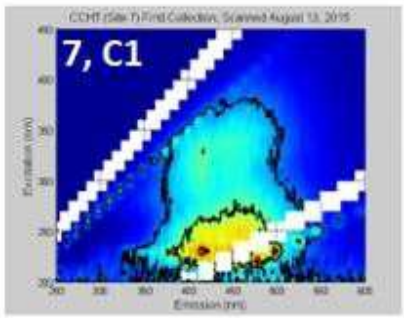
7, C1

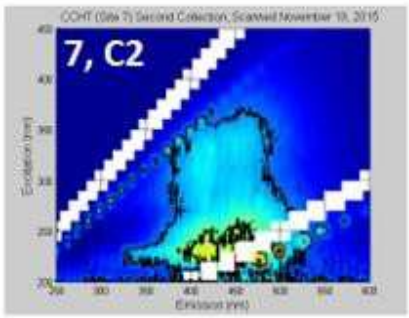
7, C2

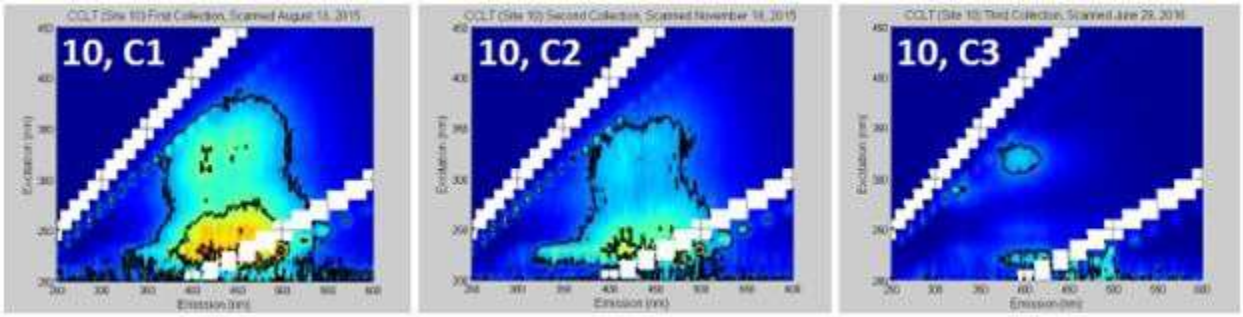

Figure 3.3: FEEMs of select east coast samples 1 (SVP), 2 (BTP), 4 (BBP), 5 (ELM), 7 (CCHT), and 10 (CCLT). Labels in upper left corners denote sample number and collection number (i.e. Collections 1, 2, and 3 are represented by 'C1', 'C2', and 'C3', respectively); x-axis is emission wavelength (nm), and y-axis is excitation wavelength (nm).

Based on the FEEMs, there were obvious fluorescence changes in samples between collection times; the intensity of the fluorescent fractions decreased in each sample between collections 1 and 2, and between 2 and 3. Areas of red and yellow were much smaller or absent by the third collection. This trend has been reported previously, where the fluorophores remain the same (and hence there is no shift in wavelength), but the signal intensity is decreased (McKnight *et al*., 2001). A possible reason for this change could be due to dilution as a result of more freshwater entering the water body, such as snow melt, rainfall, *et cetera*.

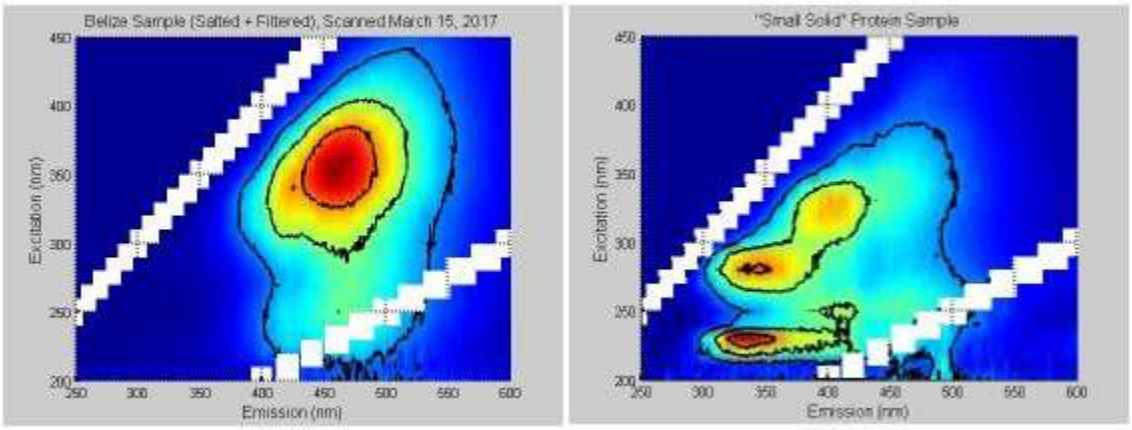

Figure 3.4: FEEMs of Belize (left) and 'Small Solid' (right) samples; x-axis is emission wavelength (nm) and y-axis is excitation wavelength (nm).

FEEMs were scanned over excitation wavelengths of 200-450 nm and emission wavelengths of 250-600 nm. All east coast samples displayed peaks in the fulvic region (Ex = 320-340 and 230 nm; Em = 400-450 nm). SVP, BTP, CCHT, and CCLT also showed fluorescence in the humic area (Ex = 360-390 or 265 nm; Em = 460-520 nm). SVP (C1 + C2), BTP (C2), ELM (C2), and CCLT (C2) suggested proteinaceous composition as well, with excitation wavelengths around 340 nm.

The Belize sample appears to be strictly humic in origin, with the most intense peak occurring at approximately Ex = 360 nm and Em = 460 nm. The 'Small Solid' protein sample appears to have humic-fulvic- and proteinaceous peaks, making it compositionally interesting. It should be noted, however, that a sample such as this would not likely be found in nature since it was the result of concentrated protein sludge mixed with MilliQ water and salted up with KMS. The strongest peaks appear in the protein region, which is expected since the sample was derived from protein skimmer waste at an aquarium store.

The FI values for each of the above samples were measured and are shown in Table 3.3. It was expected that FI values for SVP, BBP, and ELM would be lower than the others because of terrestrial input at the sample locations. This proved to be the case, and CCLT also had a low FI – likely owing to the sample being collected at low tide. BTP had sewage inputs which could be attributed to proteinaceous matter. CCHT had the highest FI of all samples, perhaps owing to the influx of autochthonous DOM from the open ocean during high tide. The Belize sample had the same FI value as BTP, and 'Small Solid' had the second highest FI of all samples. This could be explained by both samples having more autochthonous properties – Belize was collected slightly inland but near the coast, and 'Small Solid' was from saltwater tank waste (and open ocean DOM is expected to be primarily autochthonous) (Merdy *et al*., 2011).

Table 3.3: Fluorescence indices of East Coast (Blewett *et al*., 2017), Belize, and 'Small Solid' samples.

Sample	FI (Ex = 370 nm; Em = 450 nm/500 nm)
BBP	1.03
ELM	1.09
SVP	1.16
CCLT	1.17
BTP	1.35
Belize	1.35
Small Solid	1.42
CCHT	1.58

3.2.2 Fluorescence Monitoring

East coast samples from the second and third collections were scanned every few days with a portable fluorimeter as a means of monitoring changes in concentration (Figure 3.5). Both sets of samples were stored at 4°C in the dark, but third collection samples were also stored under argon. For both collections, a linear regression was run to determine whether the changes in concentration were significant. Unfortunately, concentrations changed to a significant degree (p value <0.05) for several samples from both collections (highlighted boxes in Table 3.4), and argon did not appear to help preserve the samples. Cooper *et al*. (2017) observed similar changes in samples with proteinaceous fluorophores. A more intensive storage procedure is therefore required.

Table 3.4: Linear regression results for portable fluorimeter readings; grey boxes indicate significant differences. Note that P-values were calculated for all days where data was collected.

Sample	Second Collection P-values	R^2	Third Collection P-values	R^2
SVP	0.03	0.45	0.07	0.13
BTP	0.01	0.55	<0.05	0.63
BBP	N/A	N/A	<0.05	0.56
ELM	0.21	0.19	0.03	0.19
CCHT	0.002	0.70	N/A	N/A
CCLT	0.003	0.69	0.84	0.002

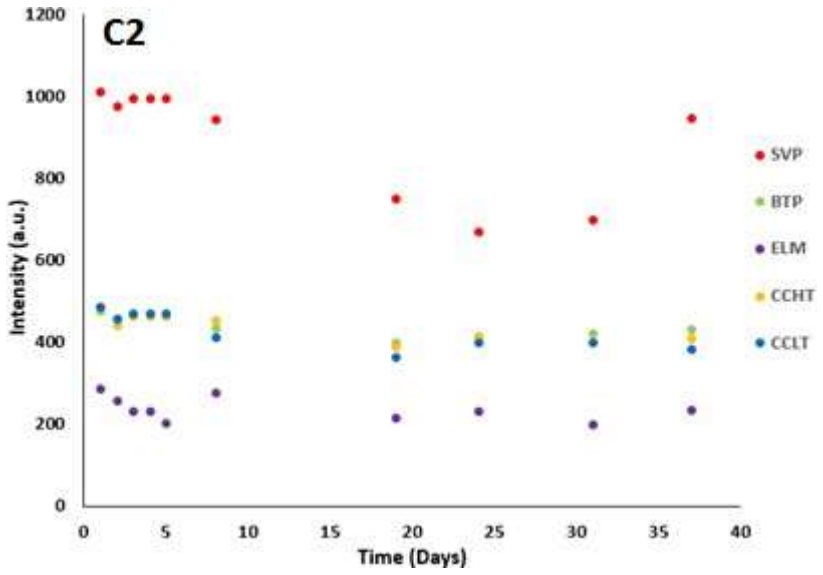

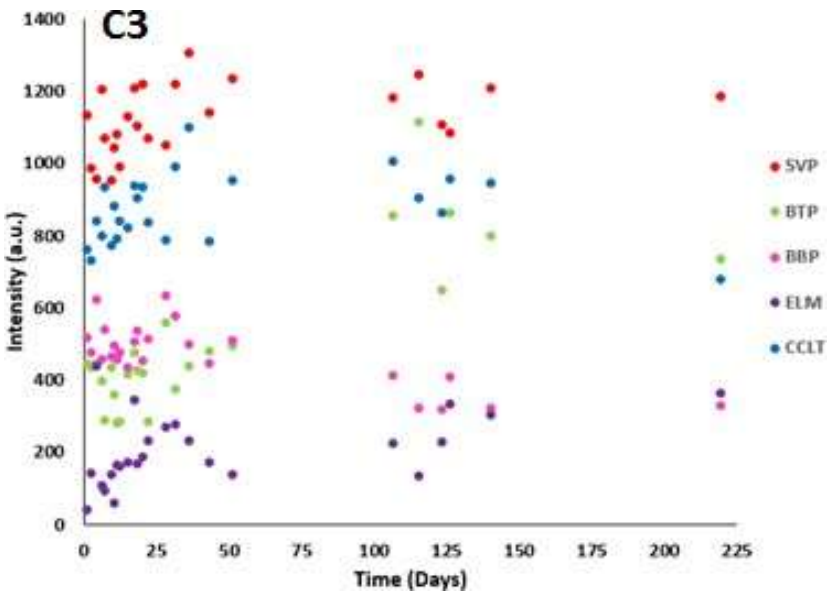

Figure 3.5: Plots of portable fluorimeter readings versus time for second east coast collection (C2) and third east coast collection (C3); x-axis is number of days, and y-axis is fluorescence intensity (au).

3.2.3 Fluorescence Quenching Titrations

A 'slice' from the FEEMs was established based on where the largest change in fluorescence intensity occurred (example FEEM with line in Figure 3.6). The corresponding excitation and emission wavelengths are shown in Table 3.5. For each sample, the respective wavelength ranges were used during the FQ titrations.

Table 3.5: Excitation and emission wavelength ranges for East Coast, Belize, and 'Small Solid' samples.

Sample	Excitation Wavelength (nm)	Emission Wavelength (nm)
SVP	200-415	250-510
BTP	200-410	250-525
BBP	200-430	250-550
ELM	205-380	250-540
CCHT	200-300	250-500
CCLT	200-410	250-525
Belize	200-440	300-550
Sm. Sol.	200-330	250-550

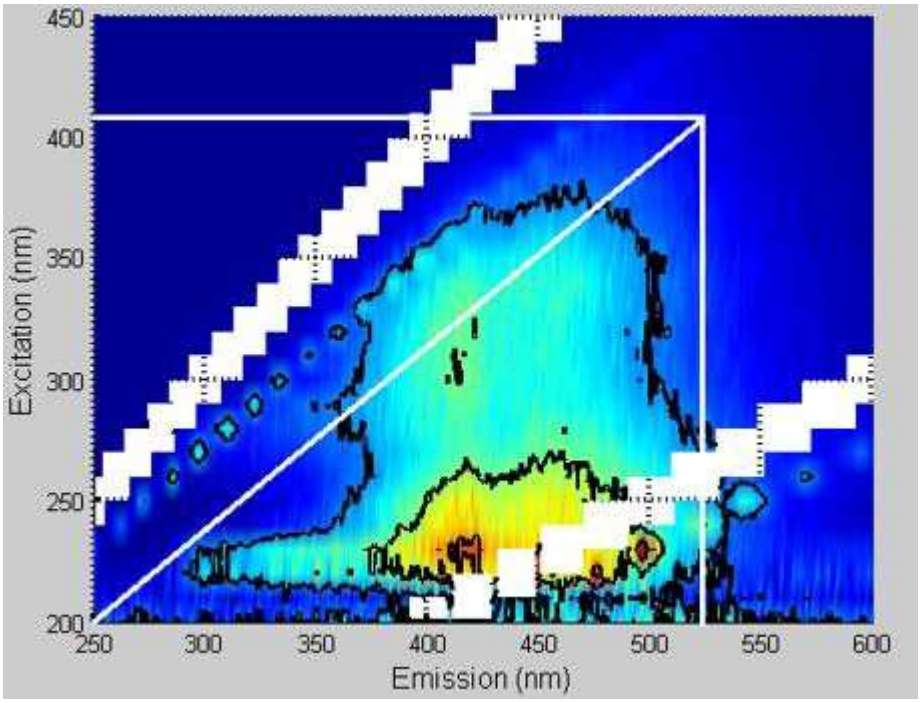

Figure 3.6: Example FEEM with 'slice' parameters, taken from this work; x-axis is emission wavelength (nm), and y-axis is excitation wavelength (nm).

The fluorescence-monitored titrations showed enhancement for BBP (Figure 3.7) and ELM, and quenching for SVP (Figure 3.7), CCHT, and Belize. Interestingly, BTP (Figure 3.8) and CCLT showed quenching for one or two of the three collections, and enhancement for the other(s); this could be due to the large decrease in fluorescence intensity between collections for these two sites.

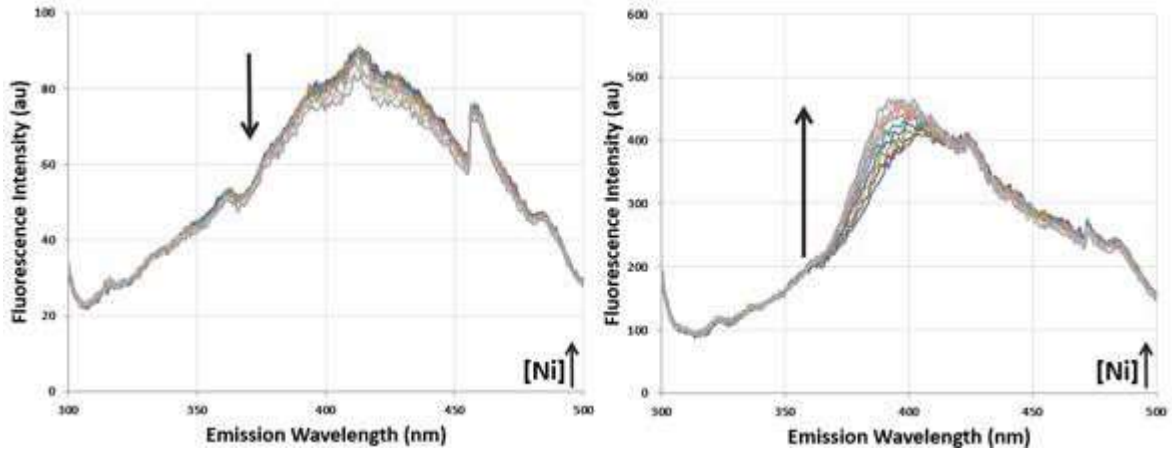

Figure 3.7: Titration of 3rd collection BBP (left), and 2nd collection SVP (right); x-axis is emission wavelength (nm), and y-axis is fluorescence intensity (au).

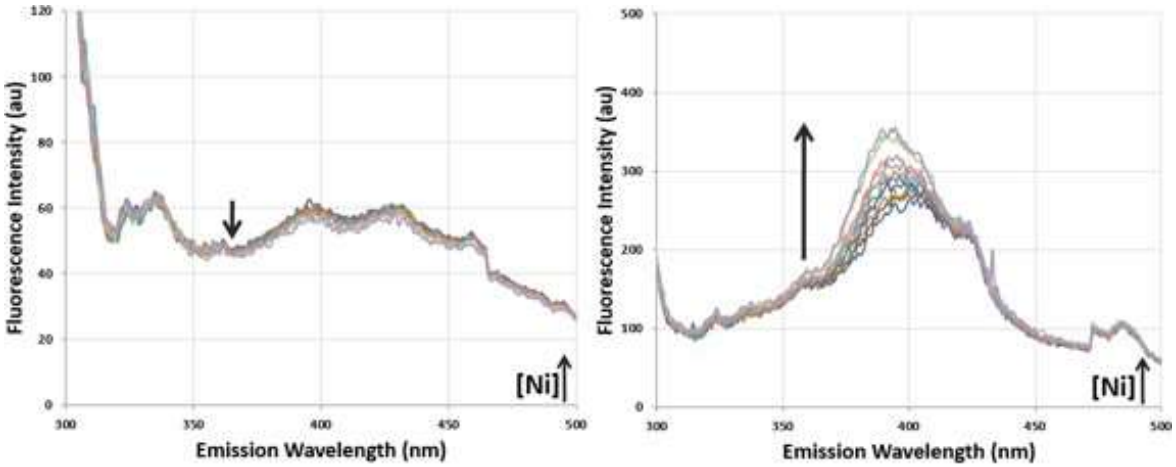

Figure 3.8: Titration of 1st collection BTP (left) versus 3rd collection BTP (right); x-axis is emission wavelength (nm), and y-axis is fluorescence intensity (au).

3.3 Quantitative Analysis

3.3.1 DOC Measurements

East coast samples from each collection, as well as the Belize grab sample, were analyzed on a Shimadzu TOC-L_{CPH} Carbon and Nitrogen Analyzer to quantify DOC (Table 3.6).

Table 3.6: Concentration of DOC in East Coast, Belize, and 'Small Solid' samples.

Sample	[DOC] (mg C/L) Coll. 1	[DOC] (mg C/L) Coll. 2	[DOC] (mg C/L) Coll. 3
SVP	4.50	4.52	2.69
BTP	3.29	2.56	1.67
BBP	2.97	N/A	3.31
ELM	2.43	1.91	0.78
CCHT	3.52	2.41	N/A
CCLT	3.35	2.36	1.07
Belize	28.91	N/A	N/A
Small Solid	27.58	N/A	N/A

The 'Small Solid' sample was made from a concentrated sludge, and so its high [DOC] is not surprising, but the Belize sample was a real sample with no prior concentration. Mangroves are rich in DOM and have been shown to contribute up to 21% of DOM in open oceans (Cawley *et al*., 2014).

3.3.2 Computational (Matlab) Analysis

After all titrations were completed, SIMPLISMA was applied to the data to solve for relative fluorophore concentrations within each sample (code in Appendix C3). Figure 3.8 is a plot of the relative concentrations of the 'pure spectra' (ie. the fluorescent fractions of the sample) derived through

SIMPLISMA for a representative sample. The topmost plot is the primary fraction detected, the middle plot is the second fraction, and the bottom plot is the third fraction, as seen by the relative amounts. It was noted that the third fraction had a relative concentration three orders of magnitude smaller than the first fraction. It also does not possess a clear peak; therefore, the code was written to account for only the first two components.

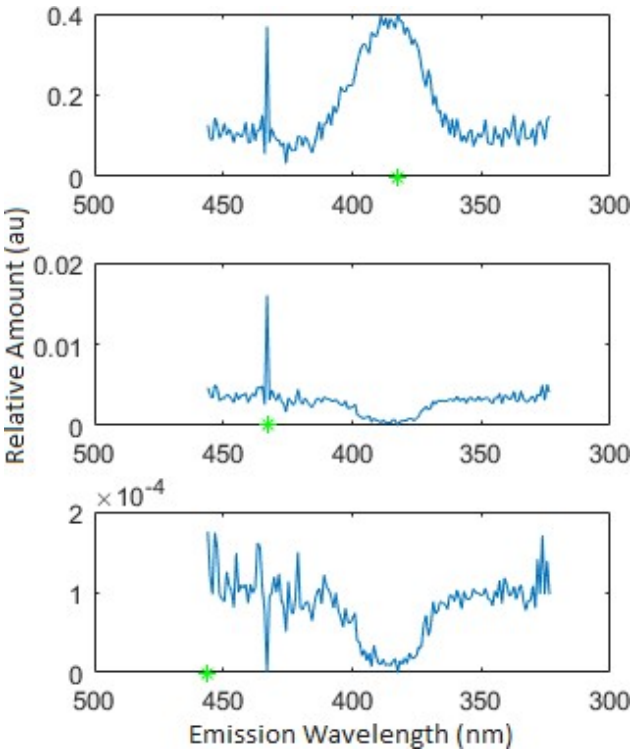

Figure 3.9: Relative amounts of pure components in sample (BTP, third collection); x-axis is emission wavelength (nm), and y-axis is relative amount (au).

These concentrations were then fit to a Ryan-Weber model, also using Matlab (code in Appendix C4) based on the log K determination described in Tait *et al*. (2016). An example of Matlab-fitted data is shown in Figure 3.10. After running the code, values for log K, L_T, and percent inefficiency were given (Table 3.7). Titrations of CCHT did not show change in fluorescence intensity, and could therefore not be fitted to the Ryan-Weber model.

Table 3.7: Results from Ryan-Weber fitting for East Coast, Belize, and 'Small Solid' samples.

Sample	Log K	Log K (2)	L_T (µmol/mg C)	L_T (2) (µmol/mg C)	% 1	% 2
SVP	6.76	5.05	0.016	0.095	0.89	0.96
BTP	6.26	6.72	0.204	0.099	1.14	0.99
BBP	6.91	6.23	0.018	0.275	1.23	0.93
ELM	7.08	6.61	0.037	0.007	1.31	0.95
CCLT	6.77	6.04	0.013	0.171	1.01	1.01
Belize	5.61	--	0.012	--	0.92	--
Sm. Sol.	6.77	--	0.002	--	0.85	--

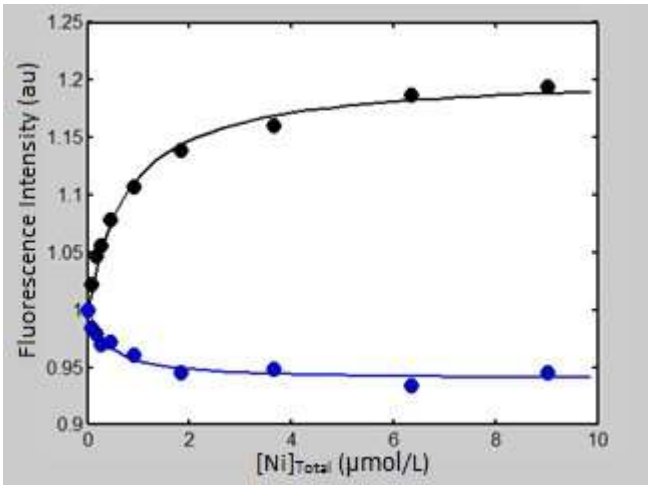

Figure 3.10: Example of data fitted to Ryan-Weber equation via Matlab; x-axis is $[Ni]_{Total}$ (µmol/L), and y-axis is fluorescence intensity (au).

While this project was underway, toxicity tests were conducted using sub-samples of the same east coast DOC collections (Blewett *et al.*, 2017). The DOC samples were used to identify possible

protective effects toward blue mussels, *Mytilus edulis*, and purple sea urchins, *Strongylocentrotus purpuratus*, against Ni toxicity. Several DOC samples showed significant protective effects (SVP, BTP, CCHT, and CCLT), and the Monte Carlo analysis outlined in Section 2.4.3 was used to quantify free Ni concentrations at the EC_{50} levels, as well as to define the 95% confidence intervals (C.I.) (Table 3.8). CCHT was not included in the comparison since it could not be fit to the Ryan-Weber model. An example of the Monte Carlo output is shown in Figure 3.11.

Table 3.8: Quantification of free $[Ni^{2+}]$ at EC_{50} levels for blue mussels (unless otherwise noted), calculated with Monte Carlo method.

Sample	**EC_{50} (µM)**	**Free $[Ni^{2+}]$ (µM)**	**St. Dev. $[Ni^{2+}]$**	**Low End of C.I. (µM)**	**High End of C.I. (µM)**
ASW	2.27	1.37	0.156	1.27	1.49
SVP	3.32	0.99	0.200	0.62	1.36
BTP	3.07	1.26	0.053	1.16	1.36
CCLT	2.90	1.15	0.074	1.01	1.28
SVP*	6.71	3.59	0.199	3.20	3.98
Belize	*2.32*	*1.27*	*0.026*	*1.22*	*1.32*
Sm. Sol.	*2.27*	*1.02*	*0.066*	*0.93*	*1.15*

*Urchin embryo results
Note: Values for Belize and 'Small Solid' samples are estimates, assuming FQ-derived speciation is correct.

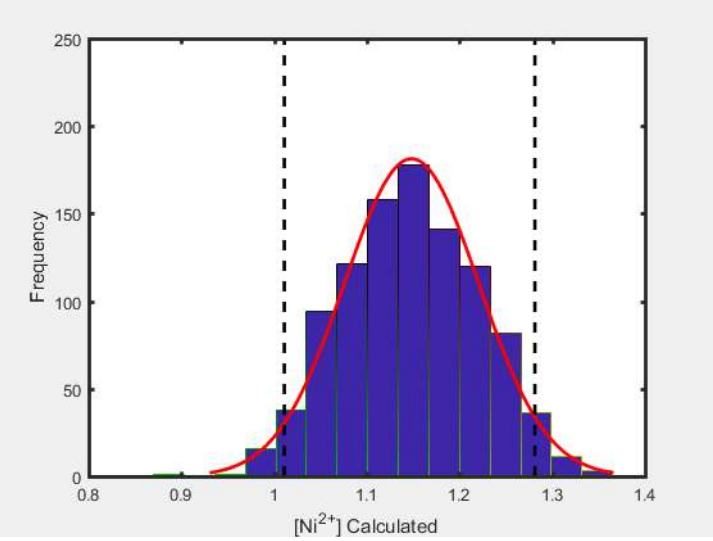

Figure 3.11: Calculated [Ni^{2+}] (in µmol Ni/L) at EC_{50} value for *Mytilus edulis* in CCLT sample.

Plots of EC_{50}'s are in Figure 3.12, and the calculated [Ni^{2+}] at the EC_{50} values based on the samples is shown in Figure 3.13. The dashed lines represent the 95% confidence interval of the ASW control in both cases.

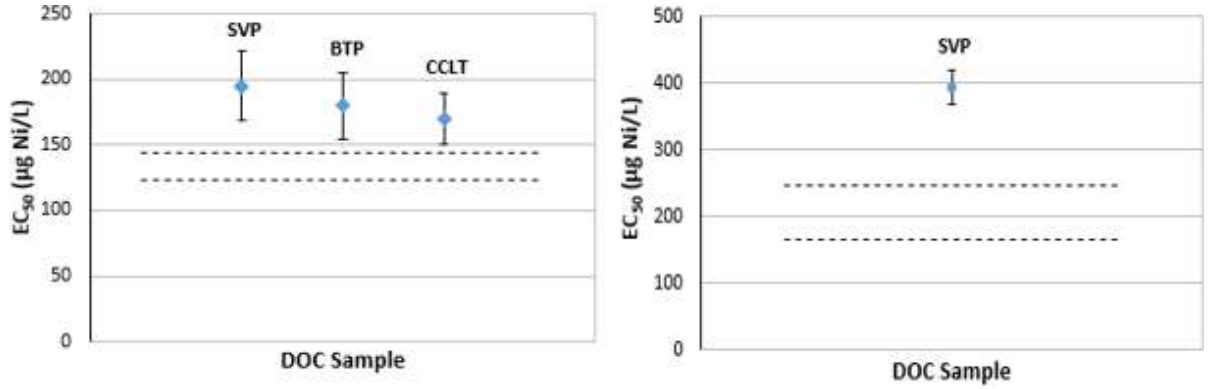

Figure 3.12: EC_{50} values for select east coast sites for *Mytilus edulis* (left) and *Strongylocentrotus purpuratus* (right); x-axis is DOC sample, and y-axis is EC_{50} in µg Ni/L.

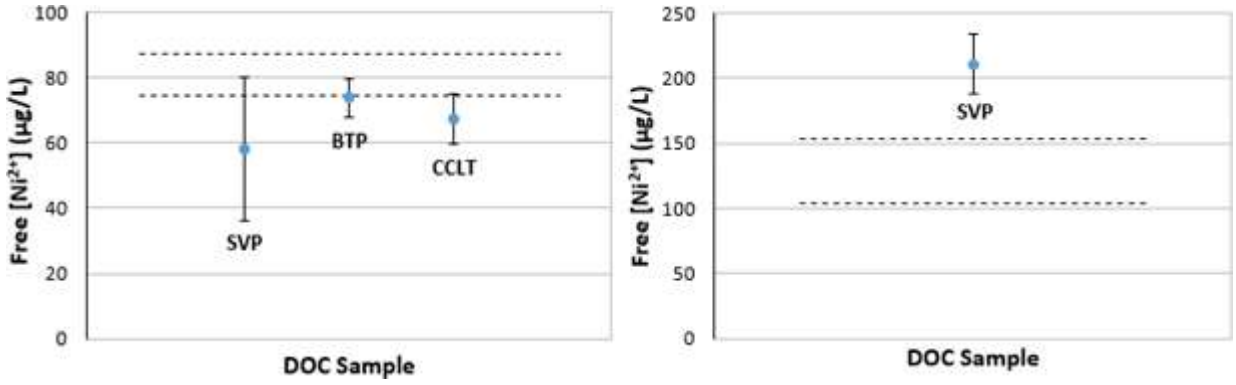

Figure 3.13: Free [Ni^{2+}] at EC_{50} values for *Mytilus edulis* (left) and *Strongylocentrotus purpuratus* (right); x-axis is DOC sample, and y-axis is free [Ni^{2+}] in µg/L.

In Figure 3.12, the samples have EC_{50} values which are significantly higher than the ASW control - this is what makes them protective (Blewett *et al*., 2017). The hypothesis that free Ni^{2+} concentrations will be constant at EC_{50} levels (and match the control) is reaffirmed in Figure 3.13 for *Mytilus edulis*. The three sites in question - SVP, BTP, and CCLT - had different properties, yet all showed the same [Ni^{2+}] at EC_{50} values (within a 95% C.I.). They also all fell within the range of [Ni^{2+}] at the EC_{50} level for ASW. Results for *Strongylocentrotus purpuratus* did not show the same relationship however, which could be due to limitations with fluorescence as a speciation technique since it only detects fluorescent ligands.

Of all samples, the most interesting was that from Belize. Without prior concentration, it had a [DOC] of nearly 30 mg C/L, and an ambient salinity of 18.34 ppt. These qualities make the sample especially relevant for studying Ni-DOM interactions in a sample that is naturally high in speciation-modifying factors. Also, because of existing and prospective Ni mines in equatorial regions for the extraction of lateritic Ni ores (Indonesia, The Philippines, et cetera), the Belize sample provided a real example of seawater DOM where Ni could have major impacts. It was disappointing, therefore, to conclude that the Belize sample did not bind as much Ni (or as strongly) as was anticipated. However, this simply highlights the need for further information on sample composition in tropical areas and possibly stricter water quality recommendations in areas where DOM is not as protective.

Chapter 4: Conclusion and Future Work

Two speciation techniques were tested in efforts to quantify free Ni in a variety of DOC samples: a Ni-ISE and fluorescence-monitored titrations. Ion-selective electrodes are a popular choice for measuring free metal ions since it is a direct speciation technique, but unfortunately a Ni ISE suitable for marine samples was not constructed during this project. The responses detected were not reproducible for dithizone membranes, and a large variation in slopes resulted while calibrating in freshwater; as well, these membranes did not respond in saltwater at all. BBTC membranes showed more reliability and gave slopes that, although not Nernstian, were consistent; they responded during titrations for multiple freshwater DOC samples, however no response was detected in salt water.

Fluorescence proved to be a reasonably strong technique, and log K values and binding capacities were determined for multiple marine samples. A Monte Carlo analysis showed that when log K and L_T values - derived from FQ titration data through Ryan-Weber analysis - were applied to $[Ni]_{Total}$ at EC_{50} levels, the predicted Ni^{2+} concentrations overlap with each other. Values for the mussel studies also overlap with the predicted free Ni^{2+} concentrations at the EC_{50} values based on the ASW blank. This confirms the hypothesis that while EC_{50} values can vary depending on water chemistry, the free Ni^{2+} concentrations remain constant. While fluorescence spectroscopy may not be a completely representative technique, it has shown to provide valuable results and may be an important tool toward Ni speciation determination.

Presently, WQG and WQC are based off of total metal concentrations, though it is recognized that dissolved fractions provide a much better understanding of toxicity toward aquatic organisms. This study has demonstrated that a connection can be made between effective concentrations and metal speciation through fluorescence data; it has highlighted that Ni-DOM complexes are quantifiable, and that fluorescence as a speciation technique can provide valuable information toward binding capacities and binding constants in real samples.

Future work should include testing other speciation measures that are more well-established, for example competitive ligand-based techniques. A reliable ISE would be ideal, so further investigation toward optimizing the response of the in-house membrane should be considered.

Developing and implementing a marine BLM for Ni is a necessary step toward stipulating appropriate water quality parameters in seawater, and being able to quantify Ni^{2+} is an important part in BLM development and has positive implications toward establishing site-appropriate WQG and WQC in marine systems.

References

Abbaspour, A.; Izadyar, A. Highly selective electrode for Nickel (II) ion based on 1.5-diphenylthiocarbazone. *Microchem. J.* **2001**, *69*, 7–11.

Baken, S.; Degryse, F.; Verheyen, L.; Merckx, R.; Smolders, E. Metal Complexation Properties of Freshwater Dissolved Organic Matter Are Explained by Its Aromaticity and by Anthropogenic Ligands. *Environ. Sci. Technol.* **2011**, *45*, 2584–2590.

Benedetti, M. F.; Van Riemsdijk, W. H.; Koopal, L. K.; Kinniburgh, D. G.; Gooddy, D. C.; Milne, C. J. Metal ion binding by natural organic matter: From the model to the field. *Geochim. Cosmochim. Acta* **1996**, *60* (14), 2503–2513.

Benner, R. Chemical composition and reactivity. In *Biogeochemistry of Marine Dissolved Organic Matter*; Hansell, D. A., Carlson, C. A., Eds.; Elsevier: USA, 2002; pp 59-90.

Birdwell, J. E.; Summers Engel, A. Characterization of dissolved organic matter in cave and spring waters using UV–Vis absorbance and fluorescence spectroscopy. *Org. Geochem.* **2010**, *41*, 270–280.

Birdwell, J. E.; Valsaraj, K. T. Characterization of dissolved organic matter in fogwater by excitation-emission matrix fluorescence spectroscopy. *Atmos. Environ.* **2010**, *44* (27), 3246–3253.

Blewett, T. A.; Glover, C. N.; Fehsenfeld, S.; Lawrence, M. J.; Niyogi, S.; Goss, G. G.; Wood, C. M. Making sense of nickel accumulation and sub-lethal toxic effects in saline waters: Fate and effects of nickel in the green crab, Carcinus maenas. *Aquat.Toxicol.* **2015**, *164*, 23–33.

Blewett, T. A.; Leonard, E. M. Mechanisms of nickel toxicity to fish and invertebrates in marine and estuarine waters. *Environ. Pollut.* **2017**, *223*, 311–322.

Blewett, T. A.; Dow, E. M.; Wood, C. M.; McGeer, J. C.; Smith, D. S. The role of dissolved organic carbon concentration and composition in ameliorating nickel toxicity to early life-stages of the blue mussel *Mytilus edulis* and purple sea urchin *Strongylocentrotus purpuratus*. *Ecotoxicol. Environ. Saf.* **2017**.

Buffle, 1977. Cited in: Aiken, G. R.; McKnight, D.; Weshaw, R. L.; MacCarthy, P. An introduction to humic substances in soil, sediment and water. John Wiley & Sons: New York, 1985; 203.

Cabaniss, S. E. Synchronous Fluorescence Spectra of Metal-Fulvic Acid Complexes. *Environ. Sci. Technol.* **1992**, *26* (6), 1133–1139.

Campbell, P. G. In *Metal Speciation and Bioavailability in Aquatic Systems*; Tessier, A. and Turner, D. R., Eds.; John Wiley & Sons: New York, 1995; pp 45-102.

Canadian Council of Ministers of the Environment. 2003. Guidance on the Site-Specific Application of Water Quality Guidelines in Canada: Procedures for Deriving Numerical Water Quality Objectives. Retrieved from http://ceqg-rcqe.ccme.ca/download/en/221.

Canadian Council of Ministers of the Environment. *A Protocol for the Derivation of Water Quality Guidelines for the Protection of Aquatic Life 2007*; 2007.

CCME (Canadian Council of Ministers of the Environment). 2008. Canadian Water Quality Guidelines. Prepared by the Task Force on Water Quality Guidelines of the Canadian Council of Ministers of the Environment.

Canadian Council of Ministers of the Environment. 2014. Water Quality Guidelines for the Protection of Aquatic Life – Freshwater, Marine. Retrieved from http://st-ts.ccme.ca/en/index.html?chems=139&chapters=all.

Cawley, K. M.; Yamashita, Y.; Maie, N.; Jaffé, R. Using Optical Properties to Quantify Fringe Mangrove Inputs to the Dissolved Organic Matter (DOM) Pool in a Subtropical Estuary. *Estuaries and Coasts.* **2014**, *37*, 399–410.

Cempel, M.; Nikel, G. Nickel: A Review of Its Sources and Environmental Toxicology. *Polish J. Environ. Stud.* **2006**, *15* (3), 385–382.

Chau, Y. K.; Kulikovsky-Cordeiro, O. T. R. Occurrence of nickel in the Canadian environment. *Environ. Rev.* **1995**, *3* (1), 95–120.

Chen, W.; Westerhoff, P.; Leenheer, J. A.; Booksh, K. Fluorescence Excitation-Emission Matrix Regional Integration to Quantify Spectra for Dissolved Organic Matter. *Environ. Sci. Technol.* **2003**, *37*, 5701–5710.

Chen, W. B.; Smith, D. S.; Guéguen, C. Influence of water chemistry and dissolved organic matter (DOM) molecular size on copper and mercury binding determined by multiresponse fluorescence quenching. *Chemosphere* **2013**, *92*, 351–359.

Chon, K.; Cho, J.; Shon, H. K. Advanced characterization of algogenic organic matter, bacterial organic matter, humic acids and fulvic acids. *Water Sci. Technol.* **2013**, *67* (10), 2228–2235.

Coble, P. G. Characterization of marine and terrestrial DOM in seawater using excitation-emission matrix spectroscopy. *Mar. Chem.* **1996**, *51* (4), 325–346.

Cooper, C. A.; Tait, T.; Gray, H.; Cimprich, G.; Santore, R. C.; McGeer, J. C.; Wood, C. M.; Smith, D. S. Influence of Salinity and Dissolved Organic Carbon on Acute Cu Toxicity to the Rotifer *Brachionus plicatilis*. *Environ. Sci. Technol.* **2014**, *48*, 1213-1221.

Cooper, C. A.; Nasir, R.; Mori, J.; McGeer, J. C.; Smith, D. S. Influence of dissolved organic carbon concentration and source on chronic 7-day Ni toxicity to the mysid, *Americamysis bahia*. *Environ. Sci. Technol.* **2017**.

Di Toro, D. M.; Allen, H. E.; Bergman, H. L.; Meyer, J. S.; Paquin, P. R.; Santore, R. C. Biotic Ligand Model of the Acute Toxicity of Metals 1. Technical Basis. *Environ. Toxicol. Chem.* **2001**, *20* (10), 2383–2396.

Doig, L. E.; Liber, K. Nickel speciation in the presence of different sources and fractions of dissolved organic matter. *Aquat. Toxicol.* **2006**, *76*, 203–216.

Duarte, R. M.; Smith, D. S.; Val, A. L.; Wood, C. M. Dissolved organic carbon from the upper Rio Negro protects zebrafish (*Danio rerio*) against ionoregulatory disturbances caused by low pH exposure. *Sci. Rep.* **2016**, *6* (1), 10.

Elias, M.; Nickel laterite deposits—geological overview, resources and exploitation. In *Giant Ore Deposits: Characteristics, Genesis, and Exploration. Centre for Ore Deposit Research Special Publication*. Cooke, D. R., Pongratz, J., Eds.; Vol. 4, pp. 205–220.

Ganjali, M. R.; Hosseini, M.; Salavati-Niasari, M.; Poursaberi, T.; Shamsipur, M.; Javanbakht, M.; Hashemi, O. R. Nickel Ion-Selective Coated Graphite PVC-Membrane Electrode Based on Benzylbis(thiosemicarbazone). *Electroanalysis.* **2002**, *14* (7–8), 526–531.

Gissi, F., *et al*., A review of nickel toxicity to marine and estuarine tropical biota with particular reference to the South East Asian and Melanesian region, Environmental Pollution (2016), http://dx.doi.org/10.1016/j.envpol.2016.08.089.

Harris, D. C. *Quantitative Chemical Analysis 8th Edition*; W. H. Freeman and Co.: New York, NY, 2010; 287-293, 309-331.

Hoatson, D. M.; Jaireth, S.; Jaques, A. L. Nickel sulfide deposits in Australia: Characteristics, resources, and potential. *Ore Geol. Rev.* **2006**, *29*, 177–241.

Hudson, N.; Baker, A.; Reynolds, D. Fluorescence Analysis of Dissolved Organic Matter in Natural, Waste and Polluted Waters - A Review. *River Res. Appl.* **2007**, *23*, 631–649.

Huguet, A.; Vacher, L.; Relexans, S.; Saubusse, S.; Froidefond, J. M.; Parlanti, E. Properties of fluorescent dissolved organic matter in the Gironde Estuary. *Org. Geochem.* **2009**, *40*, 706–719.

Johannsson, O. E.; Smith, D. S.; Sadauskas-Henrique, H.; Cimprich, G.; Wood, C. M.; Val, A. L. Photo-oxidation processes, properties of DOC, reactive oxygen species (ROS), and their potential impacts on native biota and carbon cycling in the Rio Negro (Amazonia, Brazil). *Hydrobiologia* **2017**, *789* (1), 7–29.

Kuck, P. H. Nickel. In *U.S. Geological Survey Minerals Yearbook*; 2012; p 32.

Lakowicz, J. R. *Principles of Fluorescence Spectroscopy 3rd Edition*; Springer: New York, 2006.

Lock, K.; Van Eeckhout, H.; De Schamphelaere, K. A. C.; Criel, P.; Janssen, C. R. Development of a biotic ligand model (BLM) predicting nickel toxicity to barley (*Hordeum vulgare*). *Chemosphere.* **2007**, *66*, 1346–1352.

McKnight, D. M.; Boyer, E. W.; Westerhoff, P. K.; Doran, P. T.; Kulbe, T.; Anderson, D. T. Spectrofluorometric characterization of dissolved organic matter for indication of precursor organic material and aromaticity. *Limnol. Ocean.* **2001**, *46* (1), 38–48.

Merdy, P.; Bonnefoy, A.; Martias, C.; Garnier, C.; Huclier, S. Use of fluorescence spectroscopy and voltammetry for the analysis of metal-organic matter interactions in the New Caledonia lagoon. *Int. J. Environ. Anal. Chem.* **2012**, *92* (7), 868-893.

Mudd, G. M. Global trends and environmental issues in nickel mining: Sulfides versus laterites. *Ore Geol. Rev.* **2010**, *38*, 9–26.

Niyogi, S.; Wood, C. M. Biotic Ligand Model, a Flexible Tool for Developing Site-Specific Water Quality Guidelines for Metals. *Environ. Sci. Technol.* **2004**, *38* (23), 6177–6192.

Norgate, T. E.; Jahanshahi, S.; Rankin, W. J. Assessing the environmental impact of metal production processes. *J. Clean. Prod.* **2007**, *15*, 838–848.

Nriagu, J. *Nickel in the environment*; New York: John Wiley & Sons: New York, 1980.

Nriagu, J. O. Global Metal Pollution: Poisoning the Biosphere? *Environment* **1990**, *32* (7), 7–33.

Oxley, A.; Smith, M. E.; Caceres, O. Why heap leach nickel laterites? *Miner. Eng.* **2016**, *88*, 53–60.

Packham, R.F. Studies of organic color in natural water: Proceedings of Society Water Treatment Examination, **1964**, 13, 316-334.

Pane, E. F.; Smith, C.; Mcgeer, J. C.; Wood, C. M. Mechanisms of Acute and Chronic Waterborne Nickel Toxicity in the Freshwater Cladoceran, *Daphnia magna*. *Environ. Sci. Technol.* **2003**, *37* (19), 4382–4389.

Poonkothai, M.; Shyamala Vijayavathi, B. Nickel as an essential element and a toxicant. *Int. J. Environ. Sci.* **2012**, *1* (4), 285–288.

Pretsch, E. The new wave of ion-selective electrodes. *Anal. Chem.* **2002**, *74* (15), 420A–426A.

Reck, B. K.; Müller, D. B.; Rostkowski, K.; Graedel, T. E. Anthropogenic Nickel Cycle: Insights into Use, Trade, and Recycling. *Environ. Sci. Technol.* **2008**, *42* (9), 3394–3400.

Reck, B. K.; Graedel, T. E. Challenges in Metal Recycling. *Science.* **2012**, *337*, 690–695.

Ryan, D. K.; Weber, J. H. Fluorescence Quenching Titration for Determination of Complexing Capacities and Stability Constants of Fulvic Acid. *Anal. Chem.* **1982**, *54* (6), 986–990.

Saar, R. A.; Weber, J. H. Comparison of Spectrofluorometry and Ion-Selective Electrode Potentiometry for Determination of Complexes between Fulvic Acid and Heavy-Metal Ions. *Anal. Chem.* **1980**, *52* (13), 2095–2100.

Sadiq, M. Nickel sorption and speciation in a marine environment. *Hydrobiologia.* **1989**, *176*/*177*, 225–232.

Schnebele, E. K. Nickel. *USGS Miner. Commod. Summ.* **2017**, 114–115.

Sigg, L.; Black, F.; Buffle, J.; Cao, J.; Cleven, R.; Davison, W.; Galcera, J.; Gunkel, P.; Kalis, E.; Kistlet, D.; Martin, M.; Noel, S.; Nur, Y.; Odzak, N.; Puy, J.; Van Riemsdijk, W.; Temminghoff, E.; Tercier Waeber, M.-L.; Toepperwien, S.; Town, R. M.; Unsworth, E.; Warnken, K. W.; Weng, L.; Xue, H.; Zhang, H. Comparison of Analytical Techniques for Dynamic Trace Metal Speciation in Natural Freshwaters. *Environ. Sci. Technol.* **2006**, *40* (6), 1934–1941.

Stevenson, 1982. In *An introduction to humic substances in soil, sediment and water. Humic Substances in Soil, Sediment and Water*; Aiken, G. R.; McKnight, D.; Weshaw, R. L.; MacCarthy, P., Eds.; John Wiley & Sons: New York, 1985; 203.

Smith, D. S.; Kramer, J. R. Multisite metal binding to fulvic acid determined using multiresponse fluorescence. *Anal. Chim. Acta.* **2000**, *416*, 211–220.

Smith, D. S.; Bell, R. A.; Kramer, J. R. Metal speciation in natural waters with emphasis on reduced sulfur groups as strong metal binding sites. *Comp. Biochem. Physiol. - Part C* **2002**, *133*, 65–74.

Tait, T. N.; Rabson, L. M.; Diamond, R. L.; Cooper, C. A.; McGeer, J. C.; Smith, D. S. Determination of cupric ion concentrations in marine waters: an improved procedure and comparison with other speciation methods. *Environ. Chem.* **2016**, *13*, 140–148.

Tellis, M. S.; Lauer, M. M.; Nadella, S.; Bianchini, A.; Wood, C. M. The Effects of Copper and Nickel on the Embryonic Life Stages of the Purple Sea Urchin (*Strongylocentrotus purpuratus*). *Arch. Environ. Contam. Toxicol.* **2014**, *67*, 453–464.

Templeton, D. M.; Ariese, F.; Cornelis, R.; Danielsson, L.-G.; Muntau, H.; Van Leeuwen, H. P.; Lobinski, R. Guidelines for Terms Related to Chemical Speciation and Fractionation of Elements. Definitions, Structural Aspects, and Methodological Approaches. *Pure Appl. Chem.* **2000**, *72* (8), 1453–1470.

Tessier, A.; Turner, D. R. *Metal speciation and bioavailability in aquatic systems*; John Wiley & Sons: Chichester, 1995.

Thurman, E. M.; Wershaw, R. L.; Malcolm, R. L.; Pinckney, D. J. Molecular size of aquatic humic substances. *Organic Geochemistry*. **1982**, 4, 27-35.

Thurman, E. M. *Organic Geochemistry of Natural Waters*; Dordrecht: M. Nijhoff, 1985.

Tyle, H. *Nickel*; European Union Risk Assessment Report; Denmark, 30 May 2008; 1715.

U.S. Environmental Protection Agency. 1980. Office of Water Regulations and Standards Criteria and Standards Devision. Ambient Water Quality Criteria for Nickel.

U.S. Environmental Protection Agency. 1993. Office of Water Policy and Technical Guidance on Interpretation and Implementation of Aquatic Life Metals Criteria. Retrieved from http://www3.epa.gov/npdes/pubs/owm0316.pdf.

U.S. Environmental Protection Agency. 2004. National Recommended Water Quality Criteria – Aquatic Life Criteria Table. Retrieved from http://www.epa.gov/wqc/national-recommended-water-quality-criteria-aquatic-life-criteria-table.

U.S. Environmental Protection Agency. 2015. Summary of the Clean Water Act. Retrieved from http://www.epa.gov/laws-regulations/summary-clean-water-act.

U.S. Geological Survey National Minerals Information Center staff. *USGS* **2013**, 212.

Valeur, B.; Berberan-Santos, M. N. A Brief History of Fluorescence and Phosphorescence before the Emergence of Quantum Theory. *J. Chem. Educ.* **2011**, *88*, 731–738.

Wells, M. L.; Smith, G. J.; Bruland, K. W. The distribution of colloidal and particulate bioactive metals in Narragansett Bay, RI. *Mar. Chem.* **2000**, *71*, 143–163.

Windig, W.; Heckler, C. E.; Agblevor, F. A.; and Evans, R. J. Self-modeling mixture analysis of categorized pyrolysis mass spectral data with the SIMPLISMA approach. *Chemometrics and Intelligent Laboratory Systems.* **1992**, 14: 195-207.

Wood, C. M.; Al-Reasi, H. A.; Smith, D. S. The two faces of DOC. *Aquat. Toxicol.* **2011**, *105*, 3–8.

Wood, C. M.; Farrell, A. P.; Brauner, C. J. Homeostasis and Toxicology of Essential Metals. In Fish Physiology; Farrell, A. P., Brauner, C. J., Eds.; Elsevier: London, 2012; Vol. 31A, pp 253-263.

Appendix

Figures

Codes

F1: Map of Sampling Sites in Eastern United States (Google Maps. (2015). *Rhode Island,* USA. Retrieved from https://www.google.ca/maps/place/Rhode+Island,+USA/@41.5885016,-72.5687484,145397m/data=!3m1!1e3!4m5!3m4!1s0x89e43514620ed70f:0x1e4e18bce7c106e7!8m2!3d41.5800945!4d-71.4774291. October 2015).

F2: FEEMs of all samples

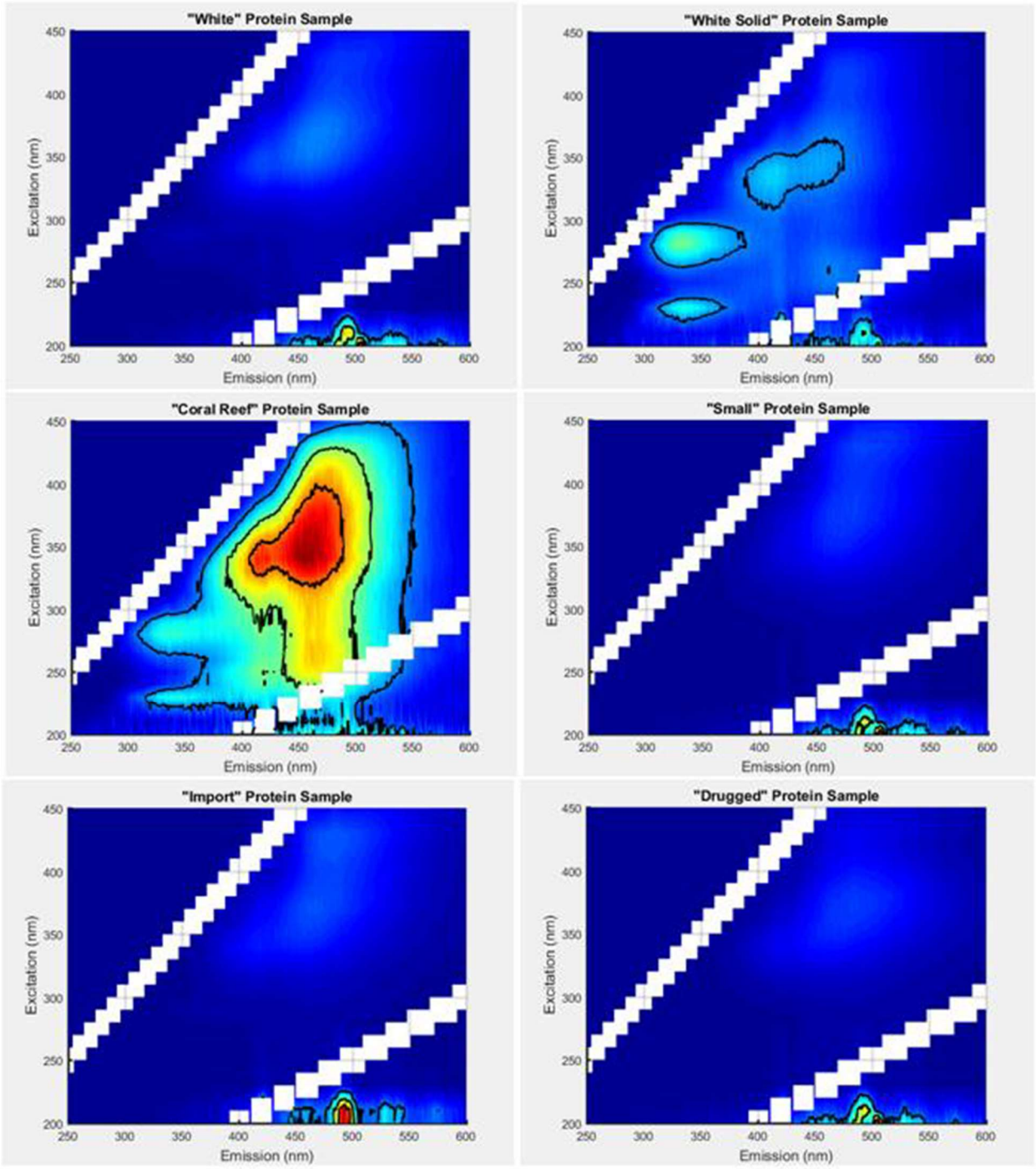

F2.1: FEEMs of other aquarium store protein skimmer waste samples.

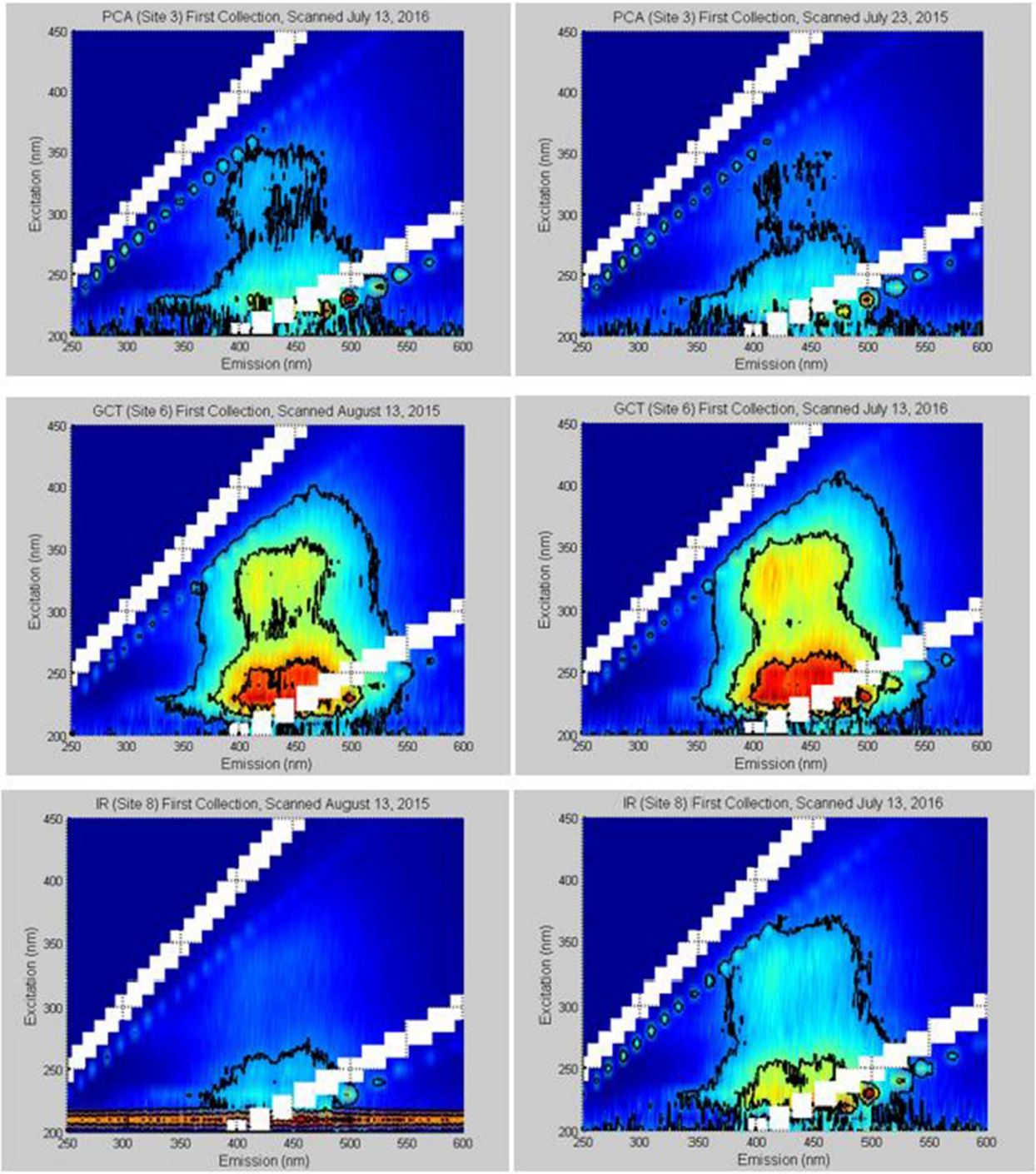
PCA (Site 3) First Collection, Scanned July 13, 2016
PCA (Site 3) First Collection, Scanned July 23, 2015
GCT (Site 6) First Collection, Scanned August 13, 2015
GCT (Site 6) First Collection, Scanned July 13, 2016
IR (Site 8) First Collection, Scanned August 13, 2015
IR (Site 8) First Collection, Scanned July 13, 2016
Excitation (nm)
Emission (nm)
200
250
300
350
400
450
500
550
600

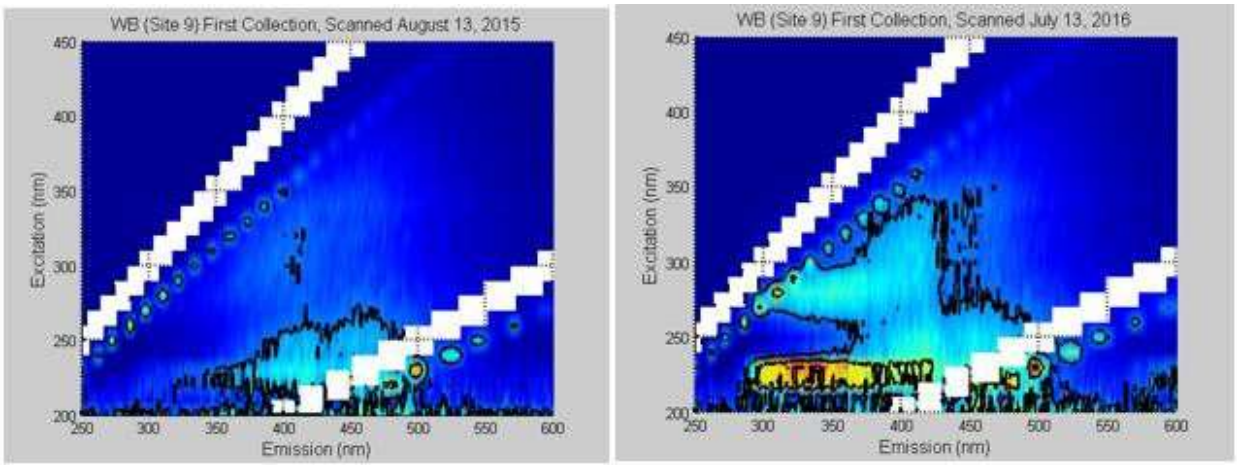

F2.2: FEEMs of other East Coast samples.

F3: All FQ titration curves

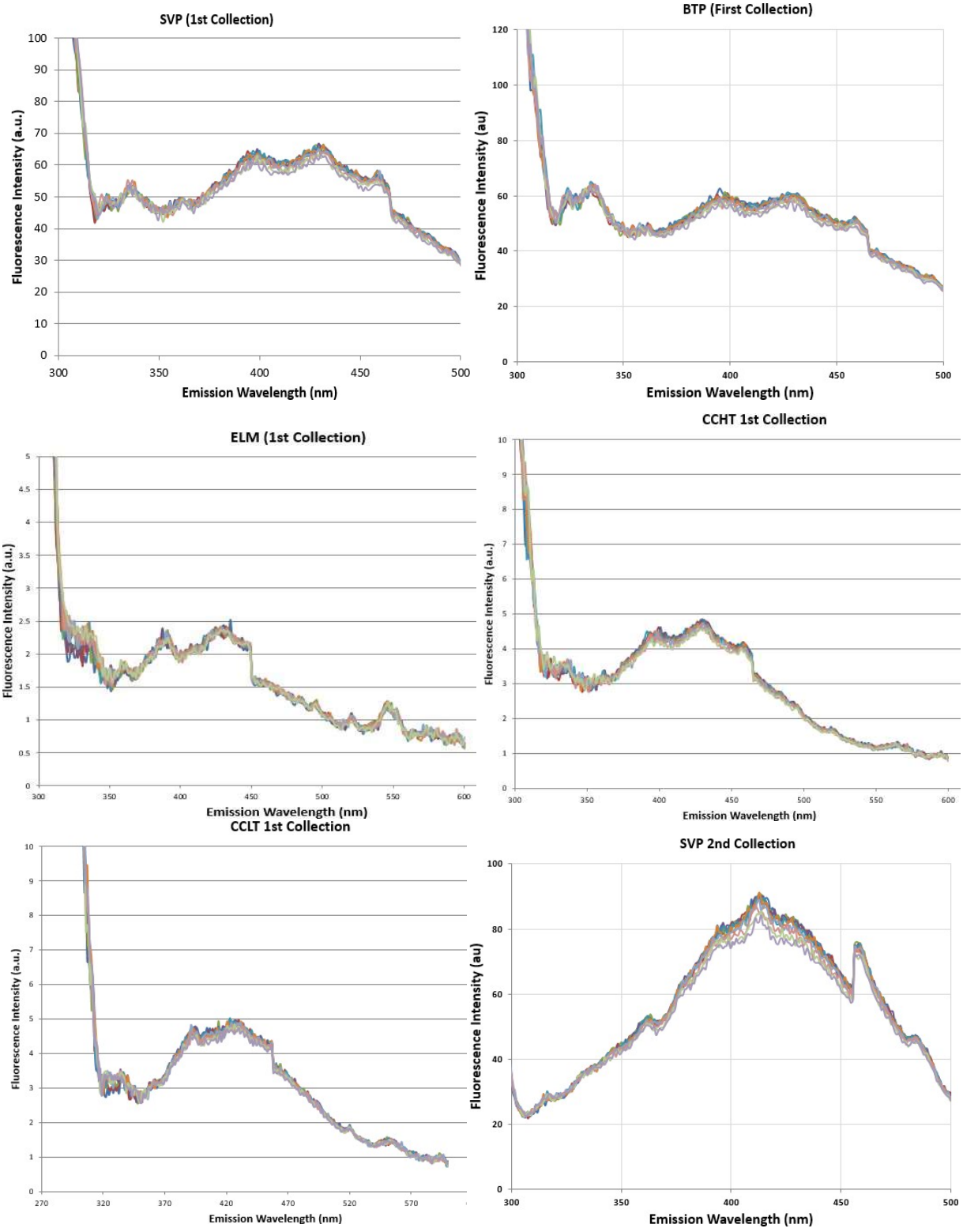

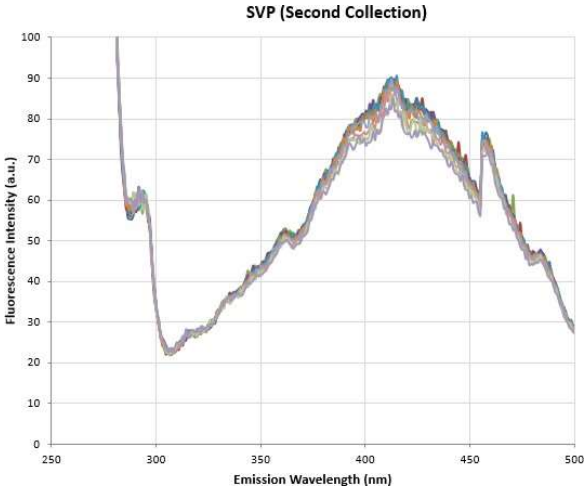
SVP (Second Collection)
Fluorescence Intensity (a.u.)
Emission Wavelength (nm)

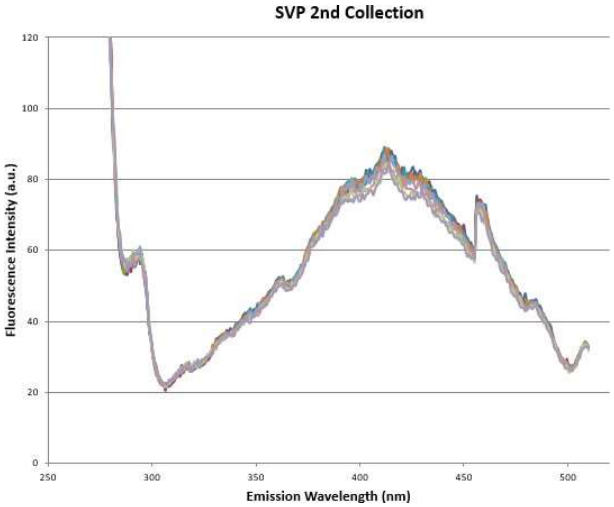
SVP 2nd Collection
Fluorescence Intensity (a.u.)
Emission Wavelength (nm)

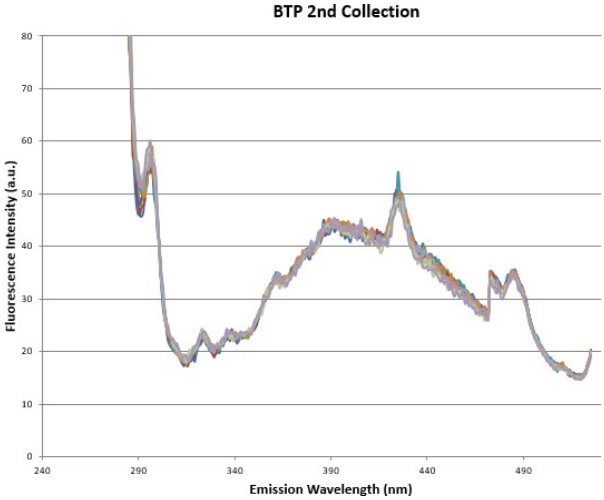
BTP 2nd Collection
Fluorescence Intensity (a.u.)
Emission Wavelength (nm)

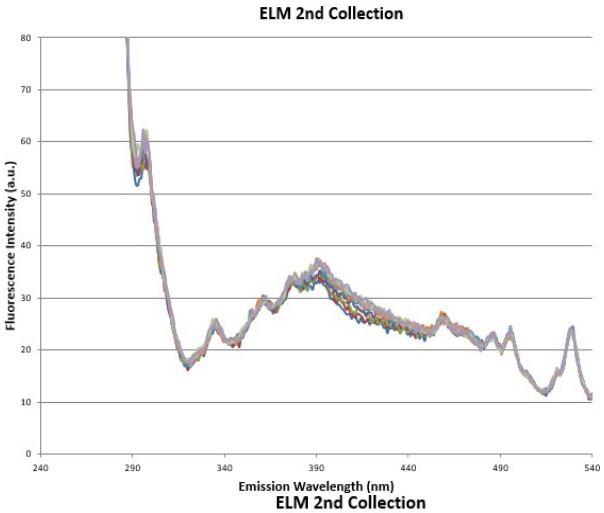
ELM 2nd Collection
Fluorescence Intensity (a.u.)
Emission Wavelength (nm)

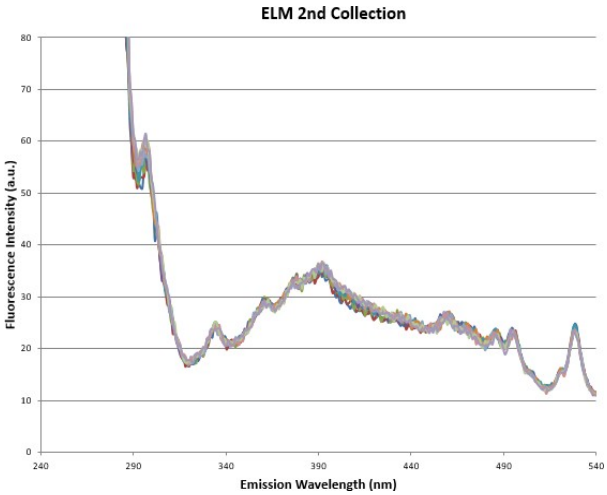
ELM 2nd Collection
Fluorescence Intensity (a.u.)
Emission Wavelength (nm)

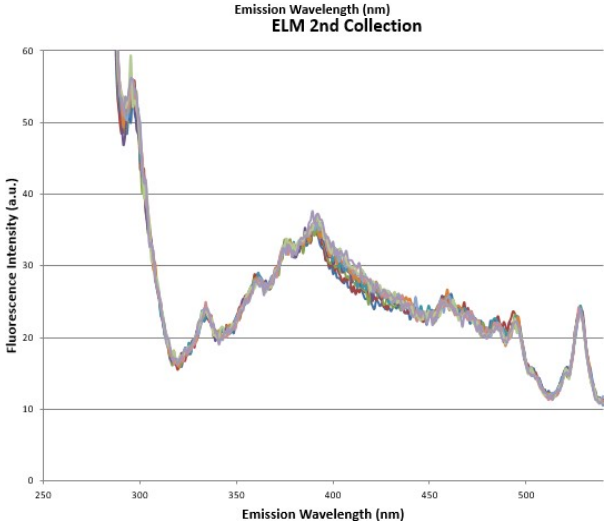
ELM 2nd Collection
Fluorescence Intensity (a.u.)
Emission Wavelength (nm)

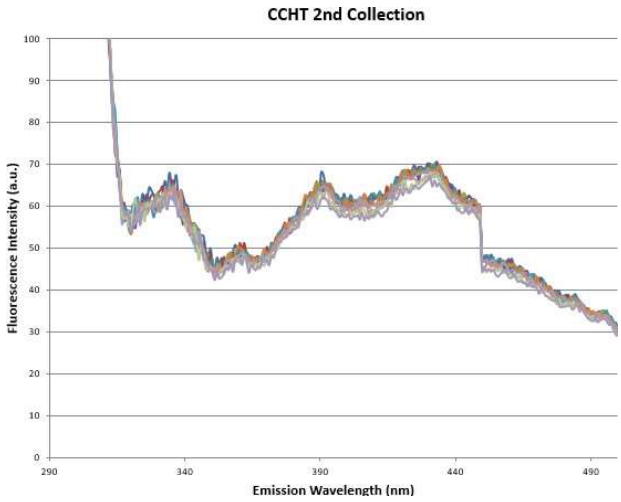
CCHT 2nd Collection
Fluorescence Intensity (a.u.)
Emission Wavelength (nm)

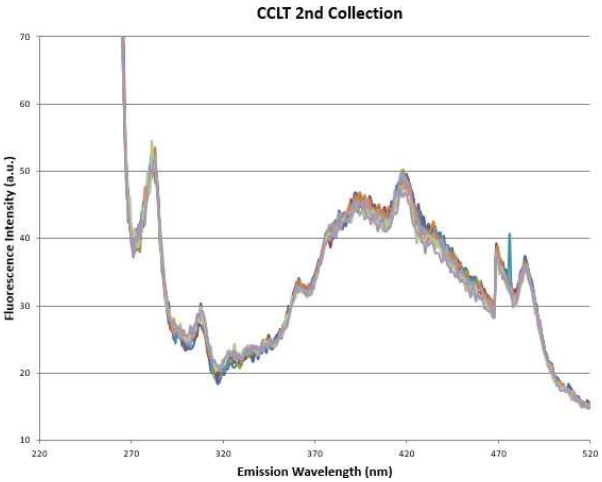
CCLT 2nd Collection
Fluorescence Intensity (a.u.)
Emission Wavelength (nm)

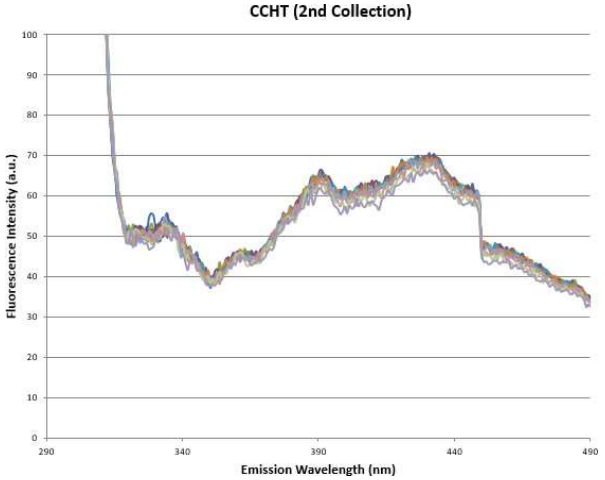
CCHT (2nd Collection)
Fluorescence Intensity (a.u.)
Emission Wavelength (nm)

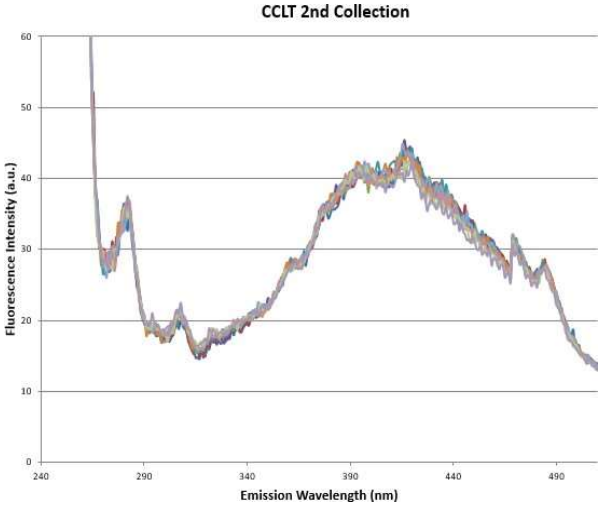
CCLT 2nd Collection
Fluorescence Intensity (a.u.)
Emission Wavelength (nm)

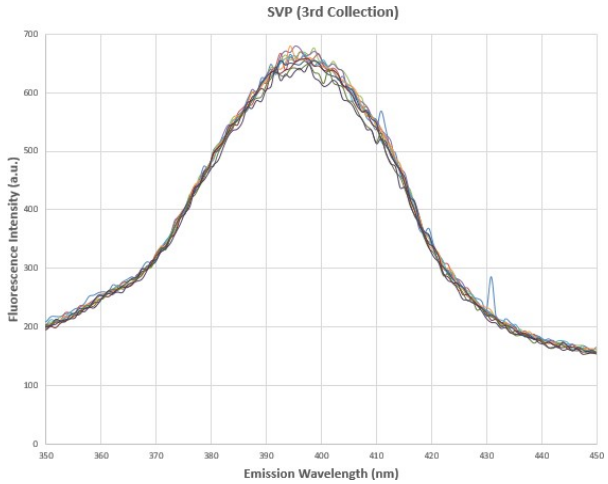
SVP (3rd Collection)
Fluorescence Intensity (a.u.)
Emission Wavelength (nm)

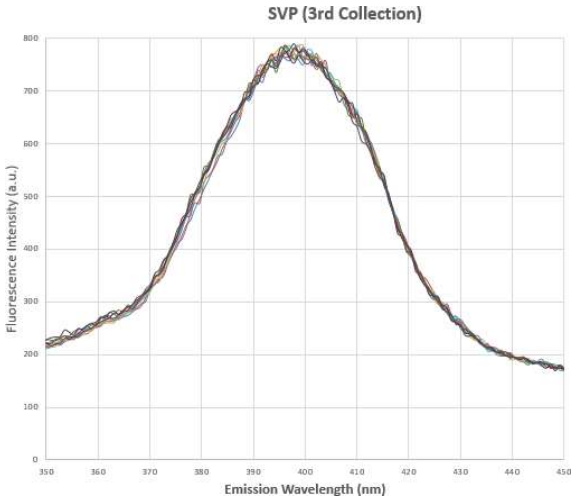
SVP (3rd Collection)
Fluorescence Intensity (a.u.)
Emission Wavelength (nm)

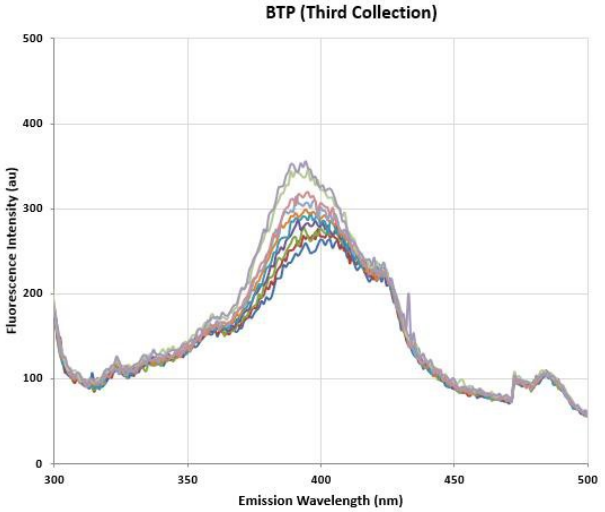
BTP (Third Collection)
Fluorescence Intensity (au)
Emission Wavelength (nm)

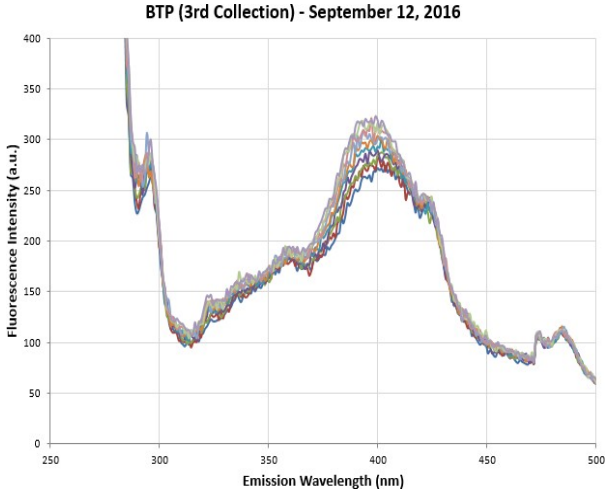
BTP (3rd Collection) - September 12, 2016
Fluorescence Intensity (a.u.)
Emission Wavelength (nm)

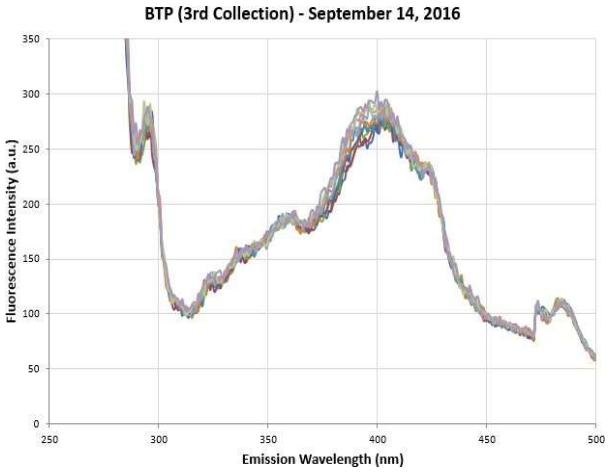
BTP (3rd Collection) - September 14, 2016
Fluorescence Intensity (a.u.)
Emission Wavelength (nm)

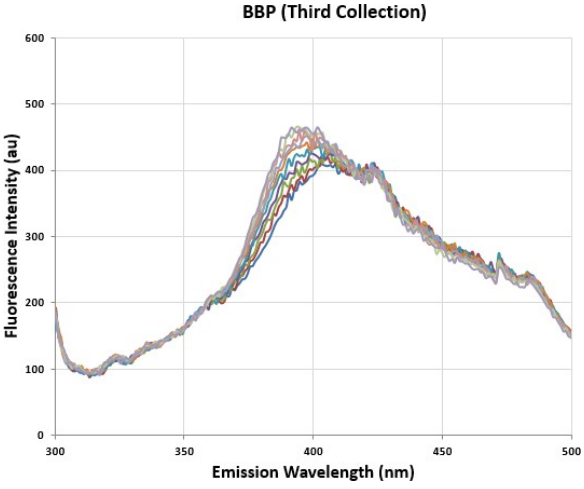
BBP (Third Collection)
Fluorescence Intensity (au)
Emission Wavelength (nm)

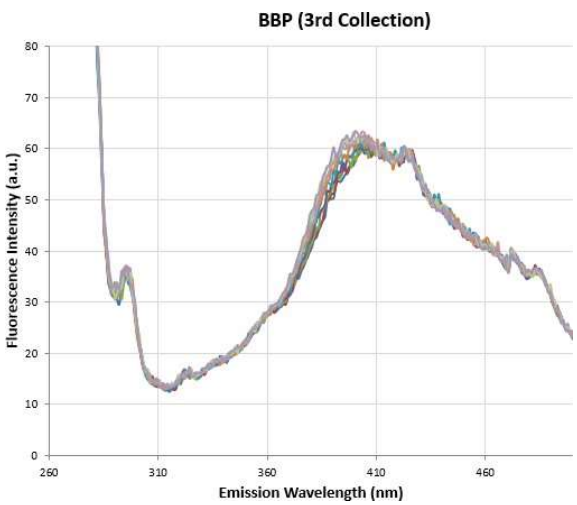
BBP (3rd Collection)
Fluorescence Intensity (a.u.)
Emission Wavelength (nm)

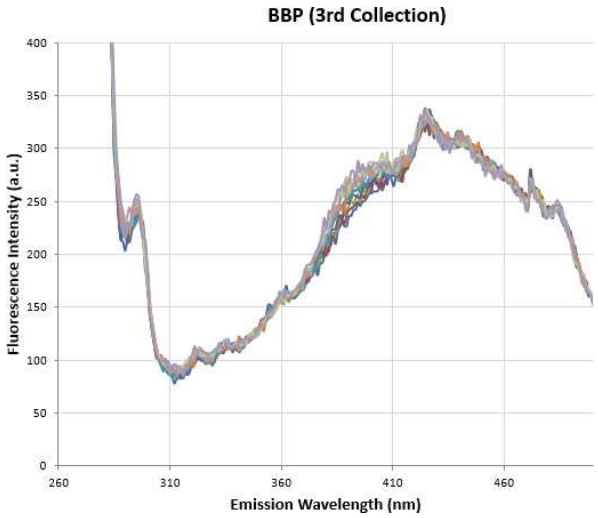
BBP (3rd Collection)
Fluorescence Intensity (a.u.)
Emission Wavelength (nm)

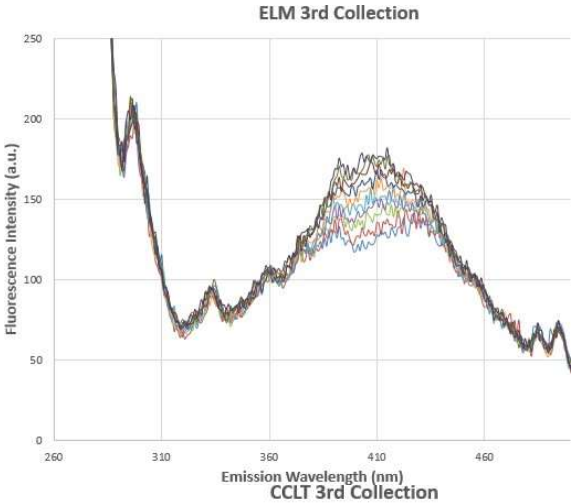
ELM 3rd Collection
Fluorescence Intensity (a.u.)
Emission Wavelength (nm)

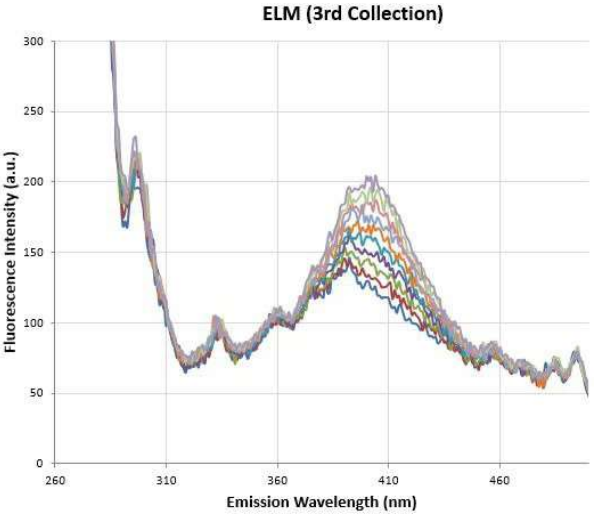
ELM (3rd Collection)
Fluorescence Intensity (a.u.)
Emission Wavelength (nm)

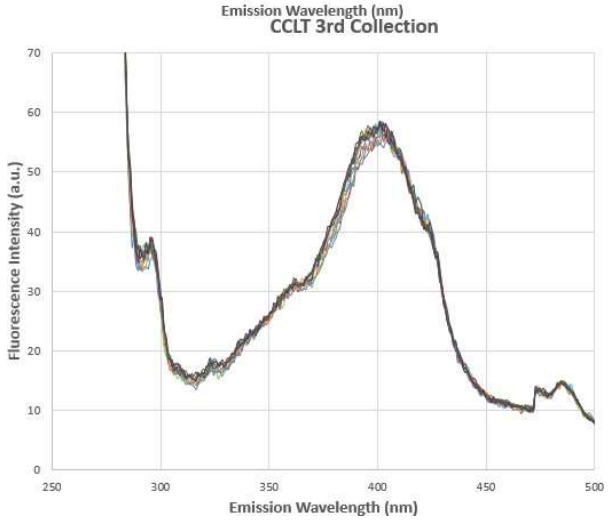
CCLT 3rd Collection
Fluorescence Intensity (a.u.)
Emission Wavelength (nm)

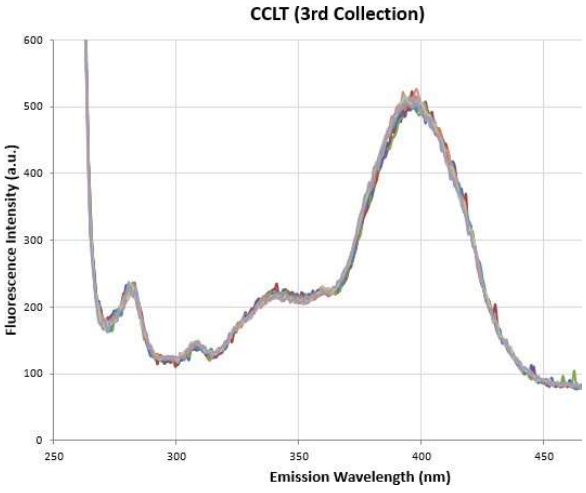
CCLT (3rd Collection)
Fluorescence Intensity (a.u.)
Emission Wavelength (nm)

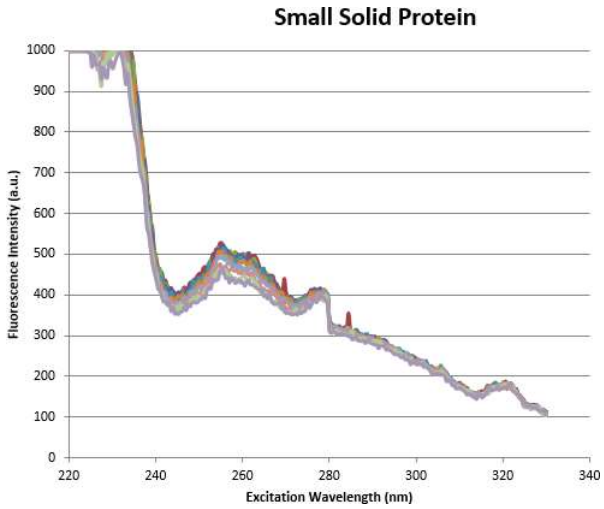
Small Solid Protein
Fluorescence Intensity (a.u.)
Excitation Wavelength (nm)

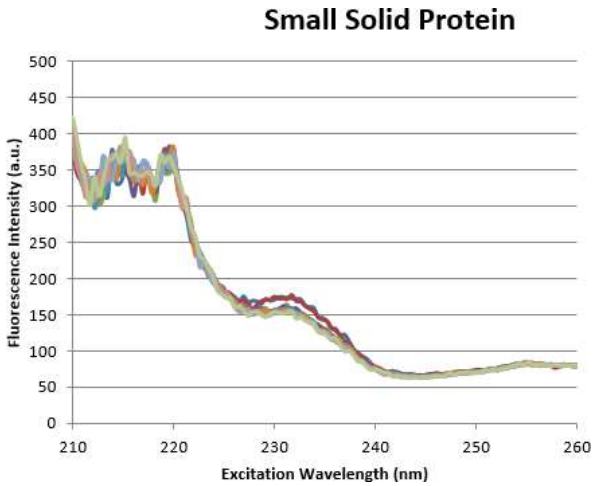
Small Solid Protein
Fluorescence Intensity (a.u.)
Excitation Wavelength (nm)

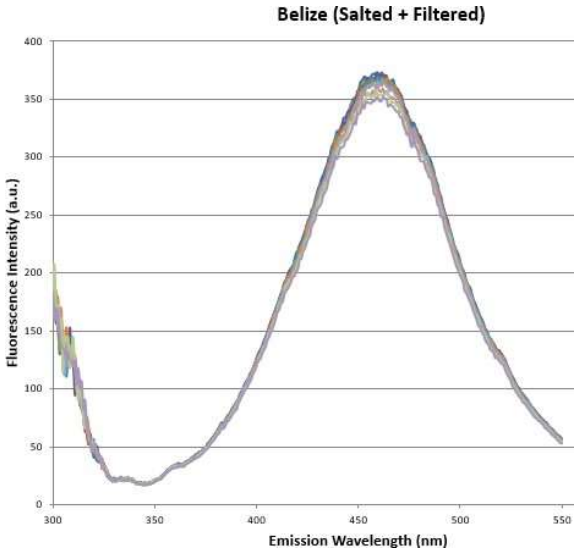
Belize (Salted + Filtered)
Fluorescence Intensity (a.u.)
Emission Wavelength (nm)

C1: MATLAB code to plot FEEM

```
function II=FEEM_code
figure(1); clf
scatterfactor=0.02;
[F,em,ex]=Fdata(scatterfactor); [Fr,emr]=resample(F,em);
makecontourplot(F,em,ex)
h=title('FEEM'); set(h,'fontsize',12)
%print Fcontour.eps -depsc2
%print Fcontour.tiff -r300 -dtiff
%print Fcontour.png -dpng
print Fcontour.jpg -djpeg
figure(2); clf
makesurfaceplot(Fr,emr,ex)
h=title('Fluorescence'); set(h,'fontsize',12)
%print Fsurf.eps -depsc2
%print Fsurf.tiff -r300 -dtiff
%print Fsurf.png -dpng
print Fsurf.jpg -djpeg
save Fname
end
function [F,em,ex]=Fdata(scatterfactor)
data=[...
200 200 210 210 220 220 230 230 240 240 250 250 260 260 270 270 280 280 290 290 300 300 310 310
320 320 330 330 340 340 350 350 360 360 370 370 380 380 390 390 400 400 410 410 420 420 430 430
440 440 450 450
% Enter raw data from spectrophotometer excel output
];
[F,em,ex]=Fprocess(data,scatterfactor);
end
function [F,em,ex]=Fprocess(data,fraction)
[N,M]=size(data)
c=0;
for i=2:2:M
        c=c+1; F(:,c)=data(2:N,i)-min(data(2:N,i));
        ex(c)=data(1,i);
end
F=F'; em=data(2:N,1); [N,M]=size(F);
em
for i=1:N
        for j=1:M
        EM=em(j);
        EX=ex(i);
        if  EM>=EX*(1-fraction)
        if EM<=EX*(1+fraction)
        F(i,j)=NaN;
        end
        end
        end
```

```
end
for i=1:N
        for j=1:M
        EM=em(j);
        EX=ex(i);
        if  EM>=(2*EX)*(1-fraction)
        if EM<=(2*EX)*(1+fraction)
        F(i,j)=NaN;
        end
        end
        end
end

end
function [G,H]=resample(data,em)
%Try to resample so things look better
[N,M]=size(data); %M is em points N is ex points. Resample every 10 nm for M
for i=1:N
        Fem=data(i,:); c=0;
        for j=1:10:M
        c=c+1; Femred(c)=Fem(j); emred(c)=em(j);
        end
        %figure(3); plot(em,Fem,'k',emred,Femred,'ko')
        %k=waitforbuttonpress
        datare(i,:)=Femred;
end
G=datare;
H=emred;
end
function makesurfaceplot(F,em,ex)
colormap('jet')
h=surf(em,ex,F)
set(gca,'linewidth',2)
view([-26 48])
axis([250 600 200 450 0 max(max(F))*1.1])
h=xlabel('Emission (nm)'); set(h,'fontsize',12)
h=ylabel('Excitation (nm)'); set(h,'fontsize',12)
h=zlabel('Intensity (arb.)'); set(h,'fontsize',12)
end
function makecontourplot(F,em,ex)
colormap('jet')
h=surf(em,ex,F)
shading interp
hold on; [C,h]=contour3(em,ex,F,3,'k'); set(h,'linewidth',2);
  set(gca,'linewidth',2)
        axis([250 600 200 450 0 max(max(F))])
view([0 90])
% hold on; plot3([250 600],[450 450],[0 0],'k','linewidth',2)
```

```
% hold on; plot3([600 600],[220 450],[0 0],'k','linewidth',2)
h=xlabel('Emission (nm)'); set(h,'fontsize',12)
h=ylabel('Excitation (nm)'); set(h,'fontsize',12)
end
```

C2: ADL code for synchronous scans
***Note: this code results in one scan, so it was entered three times to produce three scans**

```
ex_start = 200

ex_end = 440

em_start = 250

em_end = 600

num_samples = 300

delta_ex = (ex_end - ex_start)/(num_samples-1)

delta_em = (em_end - em_start)/(num_samples -1)

For sample = 0 to (num_samples-1)

current_ex = ex_start + delta_ex*sample

current_em = em_start + delta_em*sample

REM SETVAL("Goto Wavelength", current_ex)

REM SETUPINST LPRINT(current_ex, current_em, READ(current_ex, current_em) )

Next
```

C3: Code for SIMPLISMA

```
% SIMPLISMA

function II=process_titrationdata_SIMPLISMA_template

clear; figure(1); close; figure(2); close; figure(3); close; figure(4); close

data=getdata; [n,m]=size(data);

%*****************************************

lowpercent=10; highpercent=90;
%Enter percents between 0 and 100 but highpercent has be be bigger than lowpercent

%*****************************************

startdata=round(n*(lowpercent/100));

enddata=round(n*(highpercent/100)) ;

wavelength=data(startdata:enddata,1);

data=data(startdata:enddata,2:m); data=data';


figure(1); plot(wavelength,data); %k=waitforbuttonpress;

xlabel('Added Ni (ppb)','fontsize',12)

ylabel('Emission Wavelength (nm)','fontsize',12)

k=waitforbuttonpress;

%*****************************************

n=2; %Number of components

offset=0; %Value 1-15 depending on necessary correction factor

%*****************************************

varlist=[wavelength]'; % wavelengths in real spectra

[purspec,purint,purity_spec]=simplisma(data,varlist,offset,n);

figure(1); close

%*****************************************
conc=[
%Enter nominal Ni concentrations from titration
];
%*****************************************

%figure(1); plot(wavelength,purspec(1,:),wavelength,purspec(2,:),wavelength,purspec(3,:),'linewidth',2)
```

```
figure(1); plot(wavelength,purspec(1,:),wavelength,purspec(2,:),'linewidth',2)
set(gca,'linewidth',2,'fontsize',12)
xlabel('Emission Wavelength (nm)','fontsize',12)
ylabel('Pure Spectra Intensity (arb)','fontsize',12)
%Axis([340 520 0 15e-3])
print componentspectra.eps -depsc2
figure(2); close; figure(2); h=plot(conc*1e6,purint(:,1),'bo',conc*1e6,purint(:,2),'go','markersize',8)
set(h(1),'markerfacecolor','b'); set(h(2),'markerfacecolor','g')
set(gca,'linewidth',2,'fontsize',12)
xlabel('Added Ni (M*1e-6)','fontsize',12)
ylabel('Flurophore Concentration (arb)','fontsize',12)
%Axis([0 4 1.5e4 6e4])
size(conc)
size(purint)
export=[...
  conc*1e6 purint./1e4]
figure(1)
end
%*******************************************
function II=getdata
data=[...
% Enter data: first column is range of emission wavelengths; following columns are measured
% fluorescence intensities at each of the emission wavelengths
];
II=data;
end
% SIMPLISMA function
function [purspec,purint,purity_spec]=simplisma(data,varlist,offset,n,data2);
%function [purspec,purint,purity_spec]=simplisma(data,varlist,offset,n,data2);
```

```
% It is a short non interactive version of SIMPLISMA taken from Windig's article Chemometrics and
% Intelligent Laboratory Systems, 36, 1997, 3-16.

% INPUT: data contains the data matrix (spectra in rows), data 2 can be ignored or empty
% For second derivative applications data contains the conventional data and data2 contains
% the inverted 2nd data
% To create data2 use function: data2=invder(data);
% Varlist contains the variable identifiers
% Offset is a correction factor for low intensity variables (1- no offset, 15 - large offset), n is a number of
% components


% OUTPUT: purespec contains the pure spectra, purint contains the intensities ('concentrations') of the
% pure spectra in the mixtures
% purity_spec - spectra containing purity spectra
% The program will plot the purity and standard deviation spectra, where the pure variables selected
will
% be marked by a '*'. After each plot, any key needs to be pressed to continue


% INITIALIZE;

if nargin==5;

temp=data;data=data2;data2=temp;clear temp

end

[nspec,nvar]=size(data); purvarindex=[];

if nargin==4;

  data2=[];

end;

% CACULATE STATISTICS

stddata=std(data)*sqrt(nspec-1)/sqrt(nspec);

meandata=mean(data);

meandataoffset=meandata+((offset/100)*max(meandata));

lengthdata=sqrt((stddata.*stddata+meandataoffset.*meandataoffset)*...

  sqrt(nspec));

lengthmatrix=lengthdata(ones(1,nspec),:);

datalengthscaled=data./lengthmatrix;
```

```
puredata=stddata./meandataoffset;


% DETERMINE PURE VARIABLES
purity_spec=0*[1:nvar];
max_index=0;
for i=1:n+1;
 purvar=datalengthscaled(:,purvarindex);
 for j=1:nvar;
   addcolumn=datalengthscaled(:,j);
   purvartest=[purvar addcolumn];
   matrix=purvartest'*purvartest;
   weight(j)=det(matrix);
 end;
 purityspec=weight.*puredata;
          purity_spec=[purity_spec;  purityspec];
 maxindex=find(purityspec==max(purityspec));
 maxindex=maxindex(1);
%*******************************************
 % Figure 2: fluorophore concentration versus total Ni
 figure(2)
 subplot(3,2,1); plot(varlist,purityspec,'g',varlist(maxindex),...
   purityspec(maxindex),'g*');
 max_index=[max_index, maxindex];
 axis([sort([varlist(1) varlist(length(varlist))]) 0 1.1*max(purityspec)]);
 if varlist(1)>varlist(2);
   set(gca,'Xdir','reverse');
 end;
 title(['purity spectrum # ', num2str(i)]);
  stdspec=weight.*stddata;
 subplot(3,2,2);plot(varlist, stdspec,'g',varlist(maxindex),...
```

```
   stdspec(maxindex),'g*');
 axis([sort([varlist(1) varlist(length(varlist))]) 0 1.1*max(stdspec)]) ;
 if varlist(1)>varlist(2);
   set(gca,'Xdir','reverse');
 end;
title(['standard deviation spectrum # ', num2str(i)]);

%pause

  purvarindex=[purvarindex maxindex];
end
close(2)
purvarindex(n+1)=[];


%RESOLVE SPECTRA


purematrix=(data(:,purvarindex));
if isempty(data2)
purspec=purematrix\data;
else;
purspec=purematrix\data2;
end;

% RESOLVE INTENSITIES
if isempty(data2);
purint=data/purspec;
else;
purint=data2/purspec;
end;


%SCALE
```

```
if isempty(data2);
tsi=sum(data')';
else;
tsi=sum(data2')';
end;
a=purint\tsi;
purint=purint*diag(a);
purspec=inv(diag(a))*purspec;
H2.Position=[264 188 339 423];
figure(H2)
subplot(2,1,1),plot(varlist,purspec), %set(gca,'Xdir','reverse')
title ('pure spectra')
subplot(2,1,2), plot(purint), title ('pure intensity')
H3.Position=[616 190 339 423];
figure(H3)
for i=1:n+1;
  subplot(n+1,1,i), plot(abs(varlist),purity_spec(i+1,:))
  hold on, plot(abs(varlist(max_index(i+1))),purity_spec(max_index(i+1)),'g*');
  set(gca,'Xdir','reverse')
  hold off
end
end
```

C4: MATLAB code for Ryan-Weber analysis

```
% Ryan Weber fit of fluorescence data
% Needs modeltwoligandmarineNispeciation.m
function II=RyanWeber_optimization_2fluorophore_code
figure(1); clf
logK=[6.3 6.6]; LT=10.^[-6.2 -6.5];
[NiT,F1,F2]=returndata;
pguess=[logK log10(LT) 0.90 1.05]; flag=1;
% logKs logLTs then how much less efficient each fluorophore is (fraction)
% Test initial guess
error=calc2F(pguess,NiT,F1,F2,flag); k=waitforbuttonpress;
% Now optimize fminunc
% options = optimset(@fminunc);
% options = optimset(options,'Display','iter','TolFun',1e-4,'TolX',1e-3,'MaxFunEvals',1000);
% flag=0; % no plotting
% Now optimzie fminsearch (Simplex)
options = optimset(@fminsearch);
options = optimset(options,'Display','iter','TolFun',1e-1,'TolX',1e-1,'MaxFunEvals',1000);
flag=0; % no plotting
f = @(p)calc2F(p,NiT,F1,F2,flag);
[p2] = fminsearch(f,pguess,options)
%[p2] = fminunc(f,pguess,options)
% Look at best fit
figure(1); clf; flag =1; % plot it
error=calc2F(p2,NiT,F1,F2,flag);
% Compare free Ni with and without ligands
% Use 4 uM NiT for comparison
NiT=4e-6;
[Cnoligand,names]=modeltwoligandmarineNispeciation_NR(NiT,[p2(1) p2(2)],1e-20*[10^p2(3)
10^p2(4)]);
for j=1:size(Cnoligand,1)
        txt=[names(j,:),'=Cnoligand(j);'];
        eval(txt)
end
Ninoligand=Ni
[Cwithligands,SOLUTIONNAMES]=modeltwoligandmarineNispeciation_NR(NiT,[p2(1) p2(2)],[10^p2(3)
10^p2(4)]);
for j=1:size(Cwithligands,1)
        txt=[names(j,:),'=Cwithligands(j);'];
        eval(txt)
end
Niwithligand=Ni

end
function [MT,F1,F2]=returndata
data=[...
% [NiT]    F1    F2
```

```
% Enter data from SIMPLISMA anaylsis: first column is nominal concentrations of Ni added during
% titration; second and third columns are relative concentrations of fluorophores
];
conc=data(:,1)*1e-6; MT=conc; F1=data(:,2); F2=data(:,3);
end
function [C,SOLUTIONNAMES]=modeltwoligandmarineNispeciation_NR(NiT,logK,LT)
global Asolution Ksolution T
% Start by defining tableau, with two K values for two unknown ligands
K=logK; %logK of two K values
L1T=LT(1); L2T=LT(2);
[KSOLUTION,ASOLUTION,SOLUTIONNAMES]=get_equilib_defn(K);
% Reduced problem for fixed pH
pH=8.0; [Ksolution,Asolution]=get_equilib_fixed_pH(KSOLUTION,ASOLUTION,pH);
% Specify totals

ClT=0.546; NaHCO3=200; %mg/L from recipe
NaHCO3AW=100; %g/mol
CT=(NaHCO3*1e-3)/NaHCO3AW; ST=28e-3;
T=[NiT; CT; ST; ClT; L1T; L2T]; X=T;
[masserror,J,C]=nl_massbalancerrnosolid_NR(X);
end
% Equilibrium definition ----------Tableau_varymetal_fixedpHSmFQ.m
function [KSOLUTION,ASOLUTION,SOLUTIONNAMES]=get_equilib_defn(K);
%*****************************************
% H+    M   CO3   SO4  Cl   L1   L2 logK species name

Tableau=[...
1  0  0 0  0  0  0       0        {‘H'}
0  1  0 0  0  0  0       0        {'Ni'}
0  0  1 0  0  0  0       0        {'CO3'}
0  0  0 1  0  0  0       0        {'SO4'}
0  0  0 0  1  0  0       0        {'Cl'}
0  0  0 0  0  1  0       0        {'L1'}
0  0  0 0  0  0  1       0        {'L2'}
-1 0  0 0  0  0  0       -14      {'OH'}
1  0  1 0  0  0  0       9.53     {'HCO3'}
2  0  1 0  0  0  0       15.5     {'H2CO3'}
1  0  0 1  0  0  0       0.7197   {'HSO4'}
-1 1  0 0  0  0  0       -10.02   {'NiOH'}
0  1  1 0  0  0  0       3.57     {'NiCO3'}
0  1  0 1  0  0  0       0.7737   {'NiSO4'}
1  1  1 0  0  0  0       11.12    {'NiHCO3'}
0  1  0 0  1  0  0       -0.46    {'NiCl'}
0  1  0 0  0  1  0       K(1)     {'NiL1'}
0  1  0 0  0  0  1       K(2)     {'NiL2'}
];
%*****************************************

n=size(Tableau,2);
```

```
ASOLUTION=cell2mat(Tableau(:,1:n-2));
KSOLUTION=cell2mat(Tableau(:,n-1));
SOLUTIONNAMES=strvcat(Tableau(:,n));
end
% For fixed pH


function [Ksolution,Asolution]=get_equilib_fixed_pH(KSOLUTION,ASOLUTION,pH)
        [N,M]=size(ASOLUTION);
        Ksolution=KSOLUTION-ASOLUTION(:,1)*pH;
        Asolution=[ASOLUTION(:,2:M)];

end

function [F,J,C] = nl_massbalancerrnosolid_NR(X)
global Asolution Ksolution T
[Nc,Nx]=size(Asolution); %Xsolution=X(1:Nx);
criteria=1e-16;
for i=1:1000
logC=(Ksolution)+Asolution*log10(X); C=10.^(logC); % calc species
R=Asolution'*C-T;
% Evaluate the Jacobian
  z=zeros(Nx,Nx);
for j=1:Nx;
        for k=1:Nx;
        for i=1:Nc; z(j,k)=z(j,k)+Asolution(i,j)*Asolution(i,k)*C(i)/X(k); end
        end
end
J = z;
deltaX=z\(-1*R);
        one_over_del=max([1, -1*deltaX'./(0.5*X')]);
        del=1/one_over_del; X=X+del*deltaX;

        tst=sum(abs(R));
        if tst<=criteria; break; end
end

F=[R];
end
function II=calc2F(p,NiT,F1,F2,flag)
logK1=p(1); logK2=p(2); LT1=10^p(3); LT2=10^p(4);
kfracNiL1=p(5); kfracNiL2=p(6);
kL1=F1(1)/LT1; kNiL1=kfracNiL1*kL1;
kL2=F2(1)/LT2; kNiL2=kfracNiL2*kL2;
for i=1:size(NiT,1)
[C,names]=modeltwoligandmarineNispeciation_NR(NiT(i),[logK1 logK2],[LT1 LT2]);
for j=1:size(C,1)
        txt=[names(j,:),'=C(j);'];
```

```
        eval(txt)
end
vNiL1(i)=NiL1; vNiL2(i)=NiL2; vL1(i)=L1;vL2(i)=L2;
end
% For plotting

N=size(NiT,1); NiTp=min(NiT):(NiT(N)-NiT(N-1))/10:max(NiT)*1.1;
for i=1:size(NiTp,2)
[C,names]=modeltwoligandmarineNispeciation_NR(NiTp(i),[logK1 logK2],[LT1 LT2]);
for j=1:size(C,1)
        txt=[names(j,:),'=C(j);'];
        eval(txt)
end
pNiL1(i)=NiL1; pNiL2(i)=NiL2; pL1(i)=L1;pL2(i)=L2;
end
F1calcp=kL1*pL1+kNiL1*pNiL1;
F2calcp=kL2*pL2+kNiL2*pNiL2;
if flag==1;
        plot(1e6*NiTp,F1calcp./F1calcp(1),'k','linewidth',2); hold on
        plot(1e6*NiTp,F2calcp./F2calcp(1),'b','linewidth',2);
        plot(1e6*NiT,F1./F1(1),'ko','markersize',10,'markerfacecolor','k');
        plot(1e6*NiT,F2./F2(1),'ko','markersize',10,'markerfacecolor','b');
        set(gca,'linewidth',2,'fontsize',12)
end
% For error
F1calc=kL1*vL1+kNiL1*vNiL1;
F2calc=kL2*vL2+kNiL2*vNiL2;
Z=[F1calc'-F1 F2calc'-F2];
II=log10(det(Z'*Z));
end
```

C5: MATLAB code for Monte Carlo analysis

```
% Monte Carlo analysis
function II=Speciation_with_uncertainty
figure(1); clf
logK=[6.4    6.3]; logKsd=[0.2     0.3];
LT=[0.8e-6     0.5e-6]; LTsd=[0.01e-6     0.01e-6]; % in mol/L
NiT=4e-6; % in mol/L
% Put EC50 values from toxicity tests in as NiT, where applicable
for i=1:1000
LOGK=normrnd(logK,logKsd); lt=normrnd(LT,LTsd);

[Cwithligands,SOLUTIONNAMES]=modeltwoligandmarineNispeciation_NR(NiT,LOGK,lt);
for j=1:size(Cwithligands,1)
        txt=[SOLUTIONNAMES(j,:),'=Cwithligands(j);'];
        eval(txt)
end
Nicalc(i)=Ni;
end
histfit(Nicalc*1e6,15)
xlabel('[Ni^{2+}] calculated'); ylabel('frequency')
set(gca,'linewidth',2)
Nimean=mean(Nicalc)
Nisd=std(Nicalc)
dist = abs(Nicalc-Nimean);
[sortDist, sortIndex] = sort(dist);
index_95perc = sortIndex(1:floor(0.95 * numel(Nicalc)));
x_95percent = Nicalc(index_95perc);
lowend=min(x_95percent)
highend=max(x_95percent)
hold on
plot([lowend lowend]*1e6,[0 250],'k--','linewidth',2)
plot([highend highend]*1e6,[0 250],'k--','linewidth',2)

end
function [C,SOLUTIONNAMES]=modeltwoligandmarineNispeciation_NR(NiT,logK,LT)
global Asolution Ksolution T
% Start by defining tableau, with two K values for two unknown ligands
K=logK; %logK of two K values
L1T=LT(1); L2T=LT(2);
[KSOLUTION,ASOLUTION,SOLUTIONNAMES]=get_equilib_defn(K);
% Reduced problem for fixed pH
pH=8.0; [Ksolution,Asolution]=get_equilib_fixed_pH(KSOLUTION,ASOLUTION,pH);
% Specify totals
ClT=0.546; NaHCO3=200; %mg/L from recipe
NaHCO3AW=100; %g/mol
CT=(NaHCO3*1e-3)/NaHCO3AW; ST=28e-3;
T=[NiT; CT; ST; ClT; L1T; L2T]; X=T;
```

```
[masserror,J,C]=nl_massbalancerrnosolid_NR(X);
end
% Equilibrium definition ----------Tableau_varymetal_fixedpHSmFQ.m
function [KSOLUTION,ASOLUTION,SOLUTIONNAMES]=get_equilib_defn(K);
%*****************************************
% H+   M    CO3    SO4   Cl    L1   L2    logK species name

Tableau=[...
1  0   0 0   0   0   0        0         {'H'}
0  1   0 0   0   0   0        0         {'Ni'}
0  0   1 0   0   0   0        0         {'CO3'}
0  0   0 1   0   0   0        0         {'SO4'}
0  0   0 0   1   0   0        0         {'Cl'}
0  0   0 0   0   1   0        0         {'L1'}
0  0   0 0   0   0   1        0         {'L2'}
-1 0   0 0   0   0   0        -14       {'OH'}
1  0   1 0   0   0   0        9.53      {'HCO3'}
2  0   1 0   0   0   0        15.5      {'H2CO3'}
1  0   0 1   0   0   0        0.7197    {'HSO4'}
-1 1   0 0   0   0   0        -10.02    {'NiOH'}
0  1   1 0   0   0   0        3.57      {'NiCO3'}
0  1   0 1   0   0   0        0.7737    {'NiSO4'}
1  1   1 0   0   0   0        11.12     {'NiHCO3'}
0  1   0 0   1   0   0        -0.46     {'NiCl'}
0  1   0 0   0   1   0        K(1)      {'NiL1'}
0  1   0 0   0   0   1        K(2)      {'NiL2'}
];
%*****************************************

n=size(Tableau,2);
ASOLUTION=cell2mat(Tableau(:,1:n-2));
KSOLUTION=cell2mat(Tableau(:,n-1));
SOLUTIONNAMES=strvcat(Tableau(:,n));
end
% For fixed pH
function [Ksolution,Asolution]=get_equilib_fixed_pH(KSOLUTION,ASOLUTION,pH)
        [N,M]=size(ASOLUTION);
        Ksolution=KSOLUTION-ASOLUTION(:,1)*pH;
        Asolution=[ASOLUTION(:,2:M)];

end
function [F,J,C] = nl_massbalancerrnosolid_NR(X)
global Asolution Ksolution T
[Nc,Nx]=size(Asolution); %Xsolution=X(1:Nx);
criteria=1e-16;
for i=1:1000
logC=(Ksolution)+Asolution*log10(X); C=10.^(logC); % calc species
R=Asolution'*C-T;
% Evaluate the Jacobian
```

```
  z=zeros(Nx,Nx);
for j=1:Nx;
        for k=1:Nx;
        for i=1:Nc; z(j,k)=z(j,k)+Asolution(i,j)*Asolution(i,k)*C(i)/X(k); end
        end
end
J = z;
deltaX=z\(-1*R);
        one_over_del=max([1, -1*deltaX'./(0.5*X')]);
        del=1/one_over_del; X=X+del*deltaX;

        tst=sum(abs(R));
        if tst<=criteria; break; end
end
F=[R];
end
```